cmgh
CELLULAR AND MOLECULAR GASTROENTEROLOGY AND HEPATOLOGY

ORIGINAL RESEARCH

PYK2 Is Involved in Premalignant Acinar Cell Reprogramming and Pancreatic Ductal Adenocarcinoma Maintenance by Phosphorylating β-Catenin^{Y654}

Chenxi Gao,[1,2] Guangming Chen,[1,2] Dennis Han Zhang,[3] Judy Zhang,[3] Shih-Fan Kuan,[4] Wenhuo Hu,[5] Farzad Esni,[6] Xuan Gao,[1,2] Jun-Lin Guan,[7] Edward Chu,[2,8] and Jing Hu[1,2]

[1]Department of Pharmacology and Chemical Biology, [2]UPMC, Hillman Cancer Center, [4]Department of Pathology, [6]Department of Surgery, [8]Division of Hematology/Oncology, Department of Medicine, University of Pittsburgh School of Medicine, Pittsburgh, Pennsylvania; [3]Dietrich School of Arts and Sciences, University of Pittsburgh, Pittsburgh, Pennsylvania; [5]Human Oncology and Pathogenesis Program, Memorial Sloan Kettering Cancer Center, New York, New York; [7]Department of Cancer Biology, University of Cincinnati College of Medicine, Cincinnati, Ohio

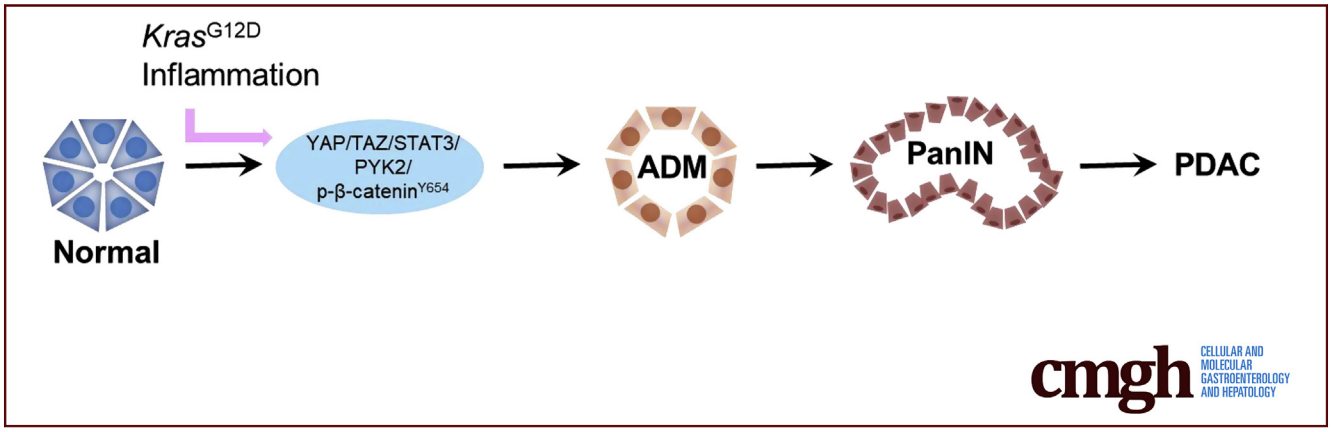

SUMMARY

By using genetically engineered mouse models molecular biology analysis, this study shows the important role of proline-rich tyrosine kinase 2 in premalignant acinar cell reprogramming and pancreatic ductal adenocarcinoma genesis. Proline-rich tyrosine kinase 2 also has been found to be required for pancreatic ductal adenocarcinoma maintenance.

BACKGROUND & AIMS: Identification and validation of new functionally relevant and pharmacologically actionable targets for pancreatic ductal adenocarcinoma (PDAC) remains a great challenge. Premalignant acinar cell reprogramming (acinar-to-ductal metaplasia [ADM]) is a precursor of pancreatic intraepithelial neoplasia (PanIN) lesions that can progress to PDAC. This study investigated the role of proline-rich tyrosine kinase 2 (PYK2) in mutant *Kras*-induced and pancreatitis-associated ADM and PanIN formation, as well as in PDAC maintenance.

METHODS: Genetically engineered mouse models of mutant *Kras* (glycine 12 to aspartic acid) and *Pyk2* deletion were used for investigating the role of PYK2 in PDAC genesis in mice. In vitro ADM assays were conducted using primary pancreatic acinar cells isolated from mice. Immunohistochemistry, immunofluorescence, and a series of biochemical experiments were used to investigate upstream regulators/downstream targets of PYK2 in pancreatic carcinogenesis. PDAC cell line xenograft experiments were performed to study the role of PYK2 and its downstream target in PDAC maintenance.

RESULTS: PYK2 was increased substantially in ADM lesions induced by mutant *Kras* or inflammatory injury. *Pyk2* deletion remarkably suppressed ADM and PanIN formation in a mutant *Kras*-driven and pancreatitis-associated PDAC model, whereas *PYK2* knockdown substantially inhibited PDAC cell growth in vitro and in nude mice. This study uncovered a novel yes-associated protein 1/transcriptional co-activator with PDZ binding motif/signal transducer and activator of transcription 3/PYK2/β-catenin regulation axis in PDAC. Our results suggest that PYK2 contributes to PDAC genesis and maintenance by activating the Wnt/β-catenin pathway through directly phosphorylating β-catenin^{Y654}.

CONCLUSIONS: The current study uncovers PYK2 as a novel downstream effector of mutant KRAS signaling, a previously unrecognized mediator of pancreatitis-induced ADM and a novel intervention target for PDAC. *(Cell Mol Gastroenterol Hepatol 2019;8:561–578; https://doi.org/10.1016/j.jcmgh.2019.07.004)*

Keywords: Acinar-to-Ductal Metaplasia; Inflammation; KRAS; Wnt/β-Catenin Signaling.

See editorial on page 651.

Pancreatic ductal adenocarcinoma (PDAC) is the fourth leading cause of cancer-related death in the United States and one of the few cancers for which survival has not improved significantly over the past 40 years. Identification of crucial factors or events required for tumor initiation/genesis and maintenance is essential for the development of effective preventive and therapeutic strategies. PDAC arises from precursor lesions called pancreatic intraepithelial neoplasms (PanINs)[1]; as a precursor of PanIN lesions, acinar-to-ductal metaplasia (ADM) is the earliest preneoplastic lesion that predisposes to PDAC.[2,3] ADM is characterized by replacement of acinar cells expressing acinar cell markers including amylase with cells expressing both acinar cell markers and ductal epithelial-specific markers, such as cytokeratin 19 (CK19).

As a crucial step in PDAC initiation, ADM can be induced by mutant *Kras*.[4–6] The *Kras* oncogene is mutated frequently in human malignancies such as colon, lung, and ovarian cancer, and the most frequent mutation is the constitutively active $Kras^{G12D}$ (glycine 12 to aspartic acid) allele. Mutations in *Kras* are found in approximately 40% of cases of human PanIN1A/1B, and in more than 90% cases of human PDAC.[7,8] It is firmly established that mutant *Kras* is a driver of PDAC initiation[9] and is required for the maintenance of pancreatic cancer in mice.[10] Despite its well-established role in PDAC, the underlying mechanisms by which oncogenic *Kras* drives PDAC initiation and progression are not fully understood and the downstream effectors of mutant *Kras* remain to be uncovered.

ADM also occurs in response to acute inflammation and commonly is observed in chronic pancreatitis.[11] Chronic pancreatitis is a significant risk factor for human PDAC and individuals with hereditary pancreatitis have a more than 50-fold increased risk for developing pancreatic cancer.[12] In mouse models of PDAC, pancreatic inflammation accelerates mutant *Kras*-induced pancreatic carcinogenesis and is essential for induction of PDAC by *Kras* in adult mice.[6,13] Pancreatitis can be induced experimentally by injection of cerulein, a cholecystokinin analogue that stimulates precocious activation of acinar cell digestive enzymes, resulting in pancreatic autodigestion and cellular damage associated with inflammation.[14] Cerulein treatment induces transient acinar cells to reprogram to form ADM lesions in wild-type mice and persistent ADM lesions in the presence of a $Kras^{G12D}$ mutation,[15,16] and greatly accelerates initiation and progression of PanIN and PDAC.[6,17] Molecular mechanisms underlying pancreatitis-induced ADM, particularly the factors or pathways mediating inflammation-triggered ADM that are druggable/targetable for disease prevention, remain to be identified.

Proline-rich tyrosine kinase 2 (PYK2) is a nonreceptor cytoplasmic tyrosine kinase. PYK2 is the only other member of the focal adhesion kinase (FAK) family with 48% amino acid identity.[18] Unlike ubiquitously expressed FAK, PYK2 expression in normal tissues is tissue- and cell type–restricted (expressed at a very low level in normal pancreas but enriched in brain and hematopoietic cells),[19] suggesting that PYK2 is not essential for normal tissue development. Indeed, mice with whole-body *Pyk2* knockout are viable and fertile, without overt impairment in development, including pancreas development or abnormal behavior.[20] Although PYK2 has been suggested to be involved in several types of cancer, the requirement of PYK2 in carcinogenesis has not yet been validated in genetically engineered mouse models of human cancer. The current study has investigated the role of PYK2 in mutant *Kras* and pancreatitis-induced ADM and PanIN formation and PDAC maintenance. Our results show that PYK2 is a novel downstream effector of mutant *Kras* signaling, a previously unrecognized mediator of pancreatitis-induced ADM and a novel preventive and therapeutic target for PDAC.

Results

PYK2 Is Overexpressed in Mutant Kras- *or Inflammatory Injury–Induced ADM Lesions*

A prior study showed that treatment with the dual FAK/PYK2 inhibitor VS-4718 substantially inhibited tumor progression, resulting in a doubling of survival in a mutant *Kras*-driven genetically engineered mouse model of PDAC,[21] suggesting that FAK, PYK2, or both FAK and PYK2 are required for PDAC carcinogenesis. This study showed that although treatment with the dual FAK/PYK2 inhibitor VS-4718 suppressed PDAC cell proliferation under 3-dimensional culture conditions, FAK knockdown failed to exert a similar effect in vitro and the inhibition occurred only when the cells were implanted in syngeneic immune-competent hosts. Although these results suggest that FAK functions mainly in stroma but not in pancreatic cancer cells, the role of PYK2 in PDAC genesis and maintenance remains to be determined.

We performed immunohistochemistry (IHC) for PYK2 on human PDAC tissue microarray containing 70 cases of PDAC tissues on the slide. Consistent with a prior study showing that PYK2 and phosphorylated PYK2 at tyrosine 402 ($p\text{-}PYK2^{Y402}$) were increased substantially in pancreatic tumors,[21] expression of PYK2 and $p\text{-}PYK2^{Y402}$ in PanINs and

Abbreviations used in this paper: **ADM, acinar-to-ductal metaplasia; CK19, cytokeratin 19; ERK1/2, extracellular signal–regulated kinase 1/2; FAK, focal adhesion kinase; FBS, fetal bovine serum; G12D, glycine 12 to aspartic acid; GSK3α/3β, glycogen synthase kinase 3α/3β; HBSS, Hank's balanced salt solution; IHC, immunohistochemistry; PanIN, pancreatic intraepithelial neoplasia; PBS, phosphate-buffered saline; PCR, polymerase chain reaction; PDAC, pancreatic ductal adenocarcinoma; PYK2, proline-rich tyrosine kinase 2; SDS-PAGE, sodium dodecyl sulfate–polyacrylamide gel electrophoresis; shRNA, short hairpin RNA; STAT3, signal transducer and activator of transcription 3; TAZ, transcriptional co-activator with PDZ binding motif; TCGA, The Cancer Genome Atlas; TGF-α, transforming growth factor α.**

Most current article

2352-345X
https://doi.org/10.1016/j.jcmgh.2019.07.004

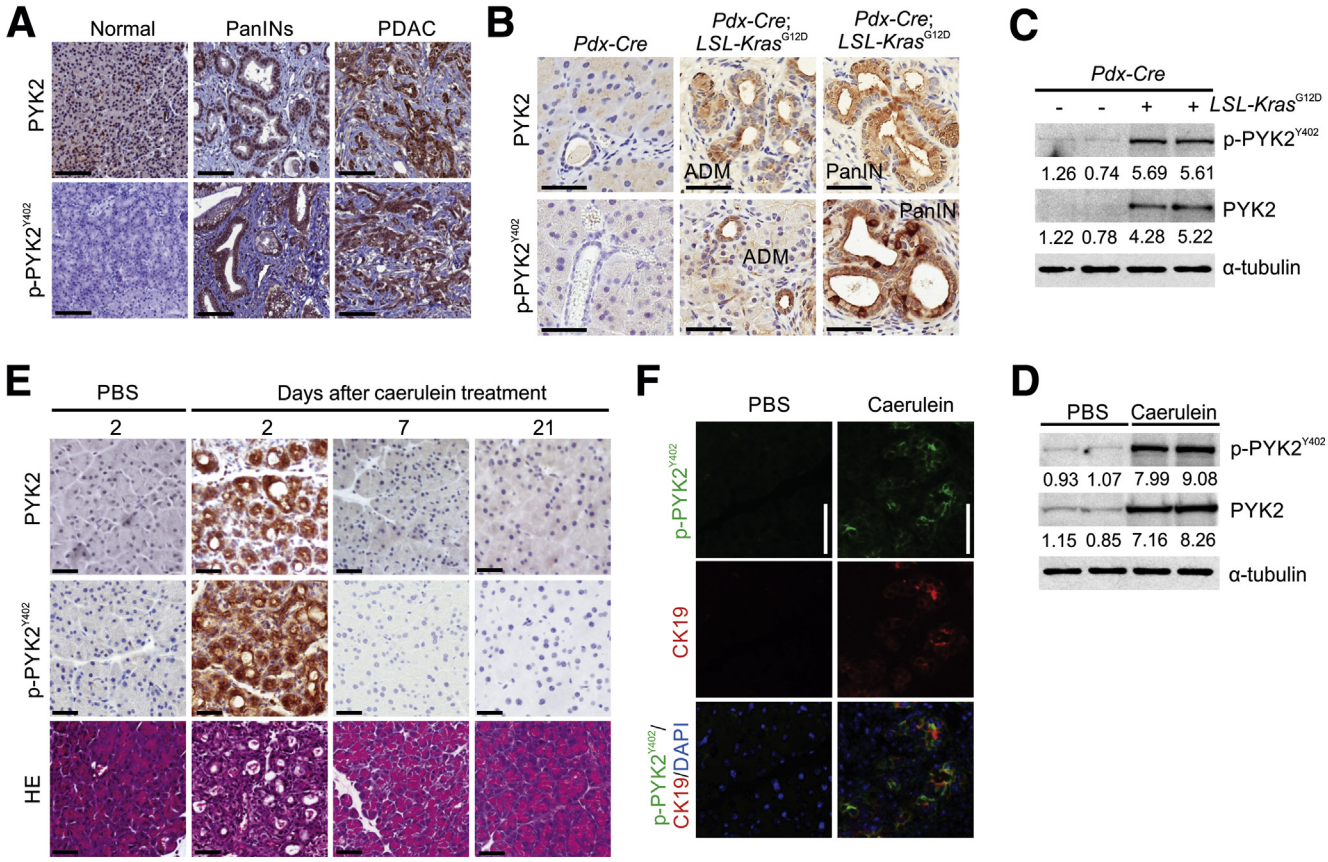

Figure 1. Hyperactivation of PYK2 in ADM and PanIN lesions. (*A*) Human PDAC tissue was stained with antibodies against PYK2 and p-PYK2^{Y402}. Representative IHC staining is shown. *Scale bars*: 100 μm. (*B*) IHC staining of PYK2 and p-PYK2^{Y402} in pancreas from 6-month-old *Pdx-Cre* mice and *Pdx-Cre*;*LSL-Kras*^{G12D} mice. *Scale bars*: 50 μm. (*C*) Immunoblotting analysis of PYK2 and p-PYK2^{Y402} levels in pancreatic tissues from *Pdx-Cre* control mice and *Pdx-Cre*;*LSL-Kras*^{G12D} mice. Each lane represents a single mouse. (*D*) *C57BL/6* mice were injected with cerulein (to induce pancreatitis) or PBS (control) for 2 consecutive days. The pancreatic tissues were collected 2 days after injection and prepared for immunoblotting analysis with indicated antibodies. (*E*) Six-week-old *C57BL/6* mice were treated with PBS or cerulein for 2 consecutive days. The pancreas was harvested at the indicated time points after injection for H&E staining and IHC staining. *Scale bars*: 50 μm. (*F*) Co-immunofluorescence staining for p-PYK2^{Y402} and CK19 in pancreatic sections from cerulein- and PBS-treated mice. *Scale bars*: 50 μm. For all panels, representative results from 3 independent experiments are shown. (*C* and *D*) The numbers under each blot represent band intensity normalized to α-tubulin and relative to expression of target proteins in *Pdx-Cre* mice or PBS-treated *C57BL/6* mice.

PDAC tumors were observed in all cases. Among the 70 cases, strong expressions of PYK2 and p-PYK2^{Y402} were noted in 48 cases (representative staining shown in Figure 1*A*), suggesting that PYK2 could be important for pancreatic carcinogenesis. Of note, p-PYK2^{Y402} represents the activated PYK2.[18] Given the hierarchy between ADM, PanINs, and PDAC, and also activation of PYK2 during pancreatic tumorigenesis (Figure 1*A*), it is likely that PYK2 activity would be increased as early as in ADMs. To test this, we evaluated PYK2 protein levels in ADM lesions induced by oncogenic *Kras* or inflammatory injury. The *Pdx-Cre*;*Lox-Stop-Lox (LSL)-Kras*^{G12D} mouse is a mutant *Kras*-driven genetically engineered mouse model of PDAC that develops PDAC with long latency and shows the full spectrum of a noninvasive precursor.[9] As expected, the IHC results showed that PYK2 and p-PYK2^{Y402} both were up-regulated in ADM and PanIN lesions in *Pdx-Cre*;*LSL-Kras*^{G12D} mice (Figure 1*B*). These results were confirmed further by Western blot analysis for PYK2 as well as p-PYK2^{Y402} on total pancreatic lysates (Figure 1*C*).

Next, we studied PYK2 expression in cerulein-induced acute pancreatitis and found high levels of PYK2 and p-PYK2^{Y402} on pancreatic lysates from *C57BL/6* mice 2 days after cerulein treatment in general (Figure 1*D*), and in ADMs in particular (Figure 1*E*). Of note, the observed activation of PYK2 was associated with ADMs, and decreased subsequently to the baseline levels as the acinar compartment recovered (Figure 1*E*). To determine the identity of the p-PYK2^{Y402}–positive cells, we performed immunofluorescence co-staining with duct cell marker CK19. Cells expressing CK19 showed high levels of p-PYK2^{Y402} (Figure 1*F*), suggesting that PYK2 is activated in the subset of cells undergoing acinar-to-ductal reprogramming upon inflammatory injury. Overall, the earlier-described results show that PYK2 is increased substantially and activated in ADM lesions induced by mutant *Kras* or inflammatory injury.

PYK2 Is Required for In Vitro ADM Formation

Activation of PYK2 in ADMs in vivo suggests that PYK2 may play a role in this process. Therefore, we next examined the ability of acinar cells to form metaplastic ducts in the absence of PYK2. To do so, primary acinar cells isolated from *LSL-Kras*^{G12D} mice or *LSL-Kras*^{G12D};*Pyk2*$^{-/-}$ mice were cultured in vitro and infected with green fluorescent protein (GFP) or Cre-recombinase expressing adenoviruses, respectively. Expression of mutant *Kras* in normal murine acinar cells is sufficient to induce ADM in primary cell culture systems.[22] As shown in Figure 2*A*, Cre-mediated activation of *Kras*^{G12D} transformed acinar cell clusters isolated from *LSL-Kras*^{G12D} mice into tubular duct-like structures. However, ADM formation was reduced significantly in acinar cell cultures originating from *LSL-Kras*^{G12D};*Pyk2*$^{-/-}$ pancreas (Figure 2*A*–*C*). The epidermal growth factor receptor ligands transforming growth factor-α (TGF-α) can drive ADM in vitro.[23–25] To confirm the requirement of PYK2 in ADM formation in the absence of oncogenic *Kras*, we isolated acinar cells from control *C57BL/6* mice and *Pyk2*$^{-/-}$ mice and cultured the cells with or without TGF-α. Here, similar to *Kras*-induced ADM, deletion of *Pyk2* appeared to prevent TGF-α–induced ADM formation as well (Figure 2*D*–*F*). The absence of CK19-positive structures further validated the inability of *Pyk2*-deficient acinar cells to undergo ADM as the result of oncogenic *Kras*-expression, or exposure to TGF-α (Figure 2*B* and *E*). Together, these findings imply that in vitro acinar-to-ductal reprogramming is PYK2-dependent.

PYK2 Is Essential for Premalignant Acinar-to-Ductal Reprogramming Induced by Mutant Kras and/or Inflammatory Injury in Mice

To investigate the role of PYK2 in ADM formation in vivo, we crossed the *Pdx-Cre*;*LSL-Kras*^{G12D} mice into a *Pyk2*$^{-/-}$ background. As expected, the pancreata of 6-week-old *Pdx-Cre*;*LSL-Kras*^{G12D} mice with cerulein treatment showed substantial CK19-positive duct structures (Figure 3*A*). However, as shown in Figure 3*A* and *B*, in the age-matched cerulein-treated *Pdx-Cre*;*LSL-Kras*^{G12D};*Pyk2*$^{-/-}$ mice, we observed a significant reduction in the number of ADMs, indicating that deletion of *Pyk2* efficiently blocked mutant *Kras*-induced premalignant acinar-to-ductal reprogramming.

To further define the requirement of PYK2 for ADM formation in an inflammatory setting in vivo, we studied cerulein-induced acute pancreatitis in *C57BL/6* mice and *Pyk2*$^{-/-}$ mice. Interestingly, although cerulein treatment caused a similar degree of acinar injury in both groups, we observed a drastic reduction in ADM formation in *Pyk2*$^{-/-}$ mice (Figure 3*C* and *D*). Together, these results prove that PYK2 is required for ADM formation induced by mutant *Kras* and/or inflammatory injury in mice.

Deletion of Pyk2 Prevents Mutant Kras-Induced PanIN Formation

Given that *Pyk2* deletion blocked oncogenic *Kras*-induced acinar-to-ductal reprogramming, we hypothesized that PYK2 is required for mutant *Kras*-driven PDAC carcinogenesis. To test this hypothesis, we examined PanIN lesions in 5- to 6-month-old *Pdx-Cre*;*Kras*^{G12D} mice, *Pdx-Cre*;*Kras*^{G12D};*Pyk2*$^{+/-}$ mice, and *Pdx-Cre*;*Kras*^{G12D};*Pyk2*$^{-/-}$ mice. At this stage, significant pancreatic area in *Pdx-Cre*;*Kras*^{G12D} mice was replaced by PanINs, as evident by Alcian blue and CK19 staining (Figure 4*A*). It is noteworthy that we found a 56% reduction in the number of PanINs in *Pdx-Cre*;*Kras*^{G12D};*Pyk2*$^{+/-}$, and a 96% reduction in *Pdx-Cre*;*Kras*^{G12D};*Pyk2*$^{-/-}$ mice, respectively (Figure 4). Our observation that *Pyk2* deletion abrogated mutant *Kras*-driven spontaneous PanIN formation implies that PYK2 may play an essential role in PanIN development in the absence of inflammatory insults. The formation of pancreatic lesions in *Pdx-Cre*;*LSL-Kras*^{G12D};*Pyk2*$^{-/-}$ mice, however, may suggest the involvement of bypass mechanisms that compensate for the loss of PYK2.

PYK2 Is Required for Mutant Kras-Driven and Pancreatitis-Associated Pancreatic Carcinogenesis

Pancreatic injury, including pancreatitis, greatly accelerates the initiation and progression of PanIN and PDAC in the presence of mutant *Kras*.[6,17] We next addressed whether PYK2 also is required for PanIN formation after pancreatic injury by evaluating the impact of *Pyk2* deletion in *Kras*-driven PanIN formation in the setting of acute pancreatitis induced by cerulein treatment. The 6-week-old mice were treated with 1 set of cerulein for 2 consecutive days. The pancreatic tissues were collected for analysis 20 days later. In a comparison with control *Pdx-Cre*;*Kras*^{G12D} mice, pancreata of *Pdx-Cre*;*Kras*^{G12D};*Pyk2*$^{-/-}$ mice showed much fewer CK19-positive duct structures (Figure 5*A*), indicating substantial reduction of PanIN lesions in *Pdx-Cre*;*Kras*^{G12D} mice with a *Pyk2* deletion (Figure 5). These results suggest that PYK2 is critical for PanIN formation after pancreatic injury in the presence of mutant *Kras*^{G12D}.

Yes-Associated Protein 1/Transcriptional Co-activator With PDZ Binding Motif/Signal Transducer and Activator of Transcription 3 Signaling Axis Mediates PYK2 Induction

PDAC frequently is associated with deregulation of crucial cancer-related signaling pathways.[26,27] The inflammatory mediator signal transducer and activator of transcription 3 (STAT3) plays a critical role in spontaneous and pancreatitis-associated PDAC genesis.[28–30] It has been reported that STAT3 binds directly to the *PYK2* promoter and regulates *PYK2* gene transcription.[31] To test whether PYK2 expression is regulated similarly by STAT3 in pancreatic cancer, we examined the effect of STAT3 inactivation on PYK2 in 2 different PDAC cell lines. As shown in Figure 6*A*, short hairpin RNA (shRNA) knockdown of *STAT3* substantially reduced PYK2 protein levels in both cell lines, confirming that STAT3 regulates PYK2 expression in PDAC cells. In mice, the IHC staining results confirmed that in the pancreatitis and pancreatic neoplasia models, the levels of phosphorylated STAT3 at tyrosine 705 (p-STAT3^{Y705}) in

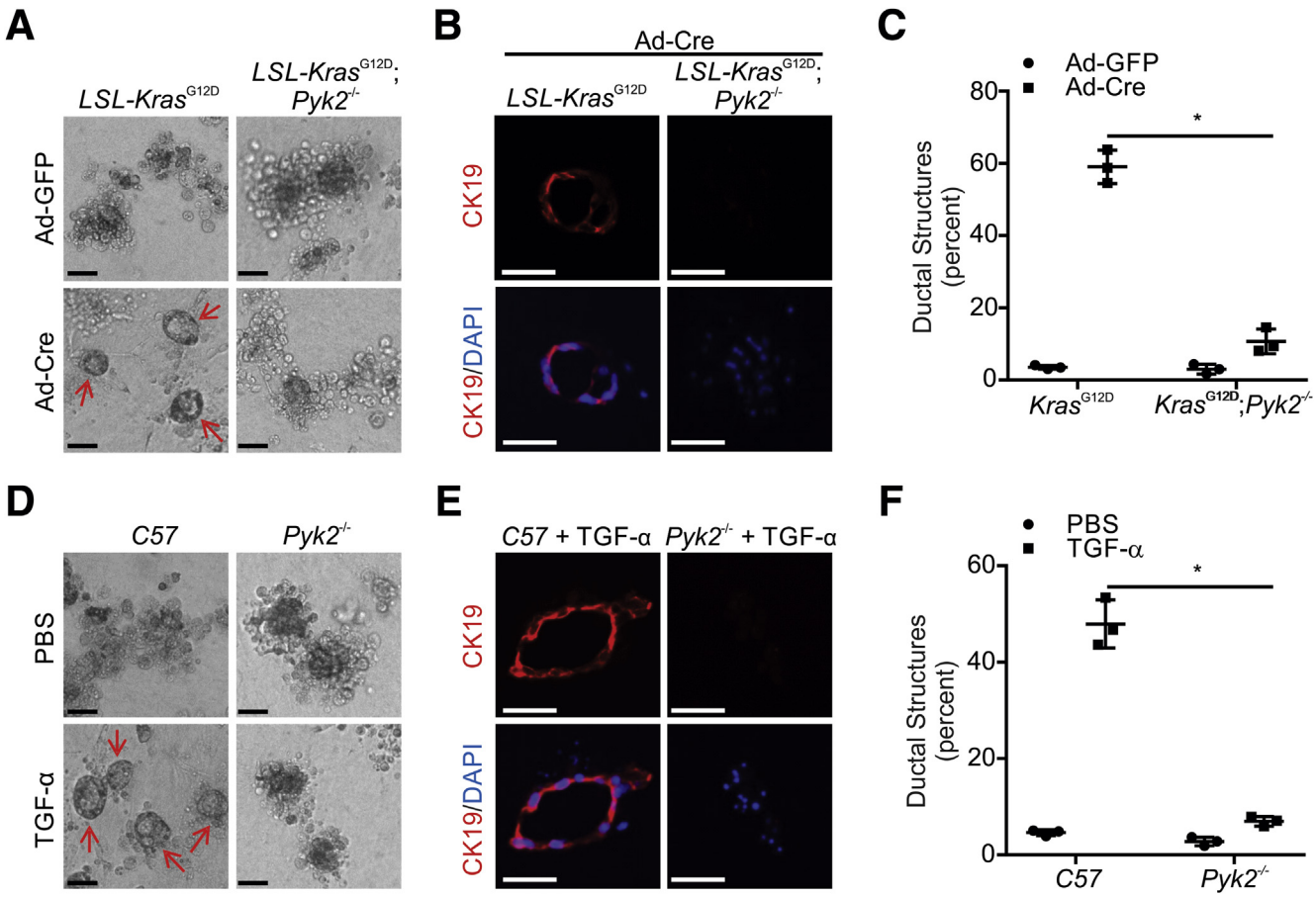

Figure 2. PYK2 is required for in vitro ADM formation. (*A*) Primary acinar cells isolated from 4-week-old *LSL-Kras*^{G12D} mice and *LSL-Kras*^{G12D};*Pyk2*$^{-/-}$ mice were infected with adenoviruses encoding either green fluorescent protein (GFP) or Cre and seeded in the 3-dimensional culture gel. Pictures were taken 5 days after seeding. Ductal-like structures (*red arrows*) were formed in acinar cells from a *LSL-Kras*^{G12D} mouse infected with Ad-Cre. *Scale bars*: 50 μm. (*B*) Immunofluorescence staining of sections from the collagen gels shown in panel *A*. The expression of CK19 in the ductal structure confirmed ADM formation. *Scale bars*: 50 μm. (*C*) Quantification of ductal structures of indicated genotypes upon indicated treatment (n = 3). Data are presented as means ± SD. *$P < .05$ (Student *t* test). (*D*) Primary acinar cells were isolated from 4-week-old *C57BL/6* mice and *Pyk2*$^{-/-}$ mice and seeded in the 3-dimensional culture gel in the presence or absence of 50 ng/mL TGF-α. Pictures were taken 5 days after seeding. *Red arrows* denote ductal structures. *Scale bars*: 50 μm. (*E*) Immunofluorescence staining of CK19 expression in sections from the collagen gels shown in panel *D*. *Scale bars*: 50 μm. (*F*) Quantification of ductal structures of indicated genotypes upon indicated treatment (n = 3). Data are presented as means ± SD. *$P < .05$ (Student *t* test). DAPI, 4′,6-diamidino-2-phenylindole.

normal acinar cells in *Pyk2*$^{+/+}$ and *Pyk2*$^{-/-}$ mice were similar. The levels of p-STAT3^{Y705} were increased in pancreatic lesions (ADM and PanINs) in *Pyk2*$^{+/+}$ and *Pyk2*$^{-/-}$ mice (Figure 6*B*), suggesting that pancreatic lesion formation does require activation of STAT3.

Hippo pathway effectors Yes-associated protein 1 (YAP) and transcriptional co-activator with PDZ binding motif (TAZ) are transcription cofactors and powerful downstream effectors of mutant KRAS in PDAC.[32–34] It has been shown that YAP and TAZ are up-regulated in pancreatitis and that they control PDAC initiation through up-regulating STAT3 signaling.[34] The YAP/TAZ/STAT3 link prompted us to investigate the possibility that up-regulation of PYK2 expression in PDAC cells occur in a YAP/TAZ-dependent manner. Thus, we next examined whether shRNA knockdown of *YAP* and *TAZ* would abrogate PYK2 expression. Our Western blot results showed that simultaneous knockdown of *YAP* and *TAZ* substantially reduced cellular levels of STAT3 and PYK2 (Figure 6*C*), implying that PYK2 expression requires YAP/TAZ in PDAC cells. In mice, the IHC staining results showed that YAP indeed was activated in pancreatic lesions (ADM and PanINs) induced by cerulein-treatment or *Kras*^{G12D} mutation, but not in normal acinar cells regardless of *Pyk2* genetic status (Figure 6*D*). Again, similar to STAT3, these findings suggest that the formation of pancreatic lesions requires activation of YAP.

Given that STAT3 binds to the *PYK2* promoter,[31] we expected that YAP/TAZ and STAT3 would regulate *PYK2* expression transcriptionally in PDAC cells. To test this, we cloned the promoter region (-2063/+113) of the *PYK2* gene, including proximal and distal promoter regions. We then compared *PYK2* promoter activities in cells transfected with scrambled shRNA or shRNA against *STAT3*, *YAP*, or *TAZ*, respectively. As shown in Figure 6*E*, *STAT3* or *YAP*/*TAZ*

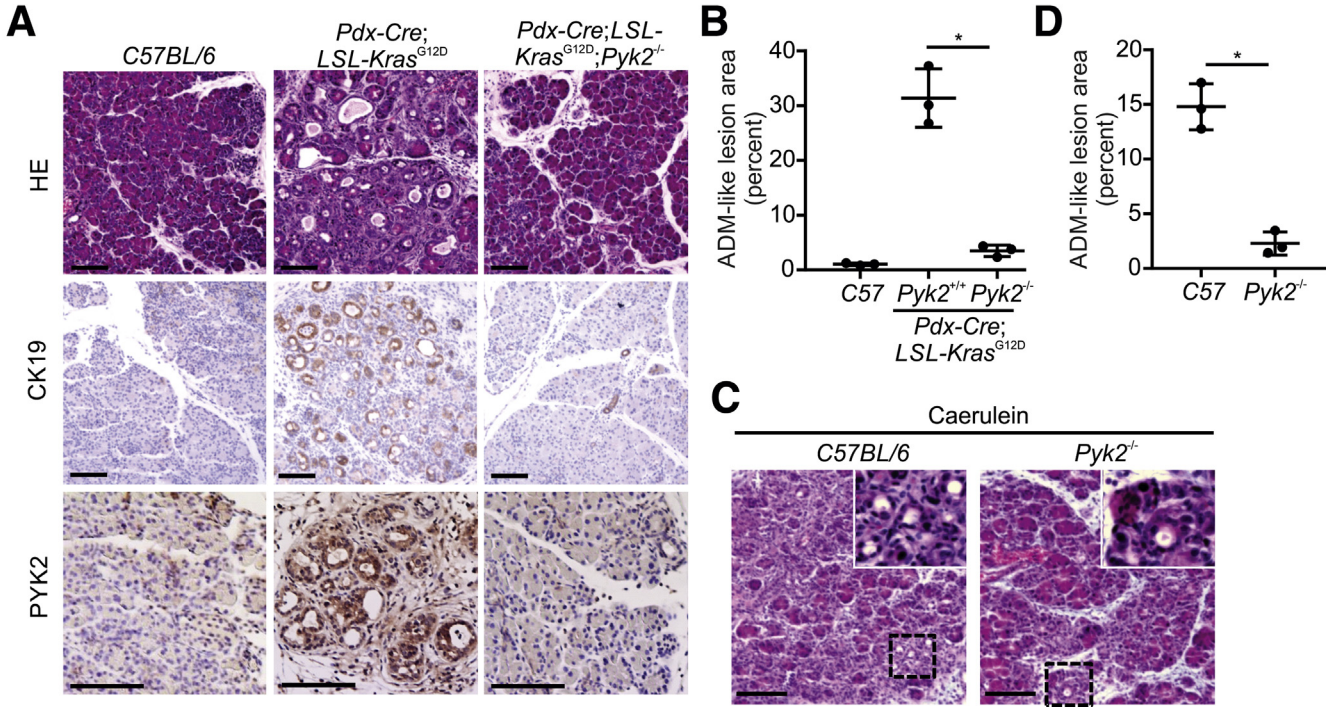

Figure 3. Mutant *Kras*- or pancreatitis-induced ADM formation requires the activation of PYK2. (*A*) Six-week-old *C57BL/6* mice, *Pdx-Cre*;*LSL-Kras*^{G12D} mice, and *Pdx-Cre*;*LSL-Kras*^{G12D};*Pyk2*$^{-/-}$ mice were injected with 1 set of cerulein for 2 consecutive days. Four days after the last treatment, the pancreatic tissues were collected and processed for H&E and IHC staining. *Scale bars*: 100 μm. (*B*) Quantification of ADM-like structures in pancreatic sections from the mice of the indicated genotypes (n = 3). Data are presented as means ± SD. *$P < .05$ (Student *t* test). (*C*) Cerulein was injected intraperitoneally into 6-week-old *C57BL/6* mice and *Pyk2*$^{-/-}$ mice to induce ADM. The pancreatic tissues were collected 3 days after the last treatment and processed for H&E staining. *Scale bars*: 100 μm. (*D*) Quantification of ADM-like structures in pancreatic sections from cerulein-treated *C57BL/6* mice and *Pyk2*$^{-/-}$ mice (n = 3). Data are presented as means ± SD. *$P < .05$ (Student *t* test).

knockdown significantly inhibited *PYK2* promoter activity in PDAC cells, confirming that STAT3 and YAP/TAZ activates *PYK2* gene transcription.

Our results suggested the existence of the YAP/TAZ/STAT3/PYK2 regulation axis in PDAC. If true, we expected to detect positive correlations between the expression levels of *YAP*, *STAT3*, and *PYK2* in human PDAC tissues. Results of analyzing The Cancer Genome Atlas (TCGA) RNA-sequencing data showed that *PYK2* expression was correlated positively with the levels of *YAP* and *STAT3* in human PDAC samples (Figure 6*F*), strongly supporting that increases of *YAP*, *STAT3*, and *PYK2* were related events in human PDAC. Overall, based on the established YAP/TAZ/STAT3 signaling axis[31,34] and the roles of these proteins in PDAC, our findings identify PYK2 as a novel downstream effector of YAP/TAZ and STAT3 in PDAC by promoting its expression.

PYK2 Phosphorylates β-Catenin at Tyrosine 654 to Activate the Wnt/β-Catenin Pathway

We next explored the molecular mechanisms mediating the role of PYK2 in PDAC. We first examined whether PYK2 exerts its role through modulating the activation of canonical mutant KRAS effectors including extracellular signal–regulated kinase 1/2 (ERK1/2) and AKT (protein kinase B, PKB).[35] The results showed that *Pyk2* deletion in *Pdx-Cre*;*Kras*^{G12D} mice did not change AKT activity (represented by phosphorylated AKT at threonine 308 [p-AKT^{T308}]), but inhibited the activities of ERK1/2 (represented by phosphorylated ERK1/2 at threonine 202/tyrosine 204 [p-ERK1/2$^{T202/Y204}$]) and RAS (represented by RAS-Guanosine-5'-triphosphate [RAS-GTP]) (Figure 7*A*), suggesting that PYK2 could function through regulating KRAS and ERK activity. It is well established that the levels of active RAS must reach a threshold to achieve transformation,[36] and that increasing the levels of active RAS causes more rapid transformation.[37] That said, we believe that down-regulation of RAS activity contributed largely to *Pyk2* deletion-mediated inhibition of PDAC genesis.

In an effort to search for other PYK2 effectors, we reasoned that PYK2, as a cytoplasmic tyrosine kinase, is involved in PDAC carcinogenesis through phosphorylating downstream substrate(s), which plays an important role in PDAC genesis. Wnt/β-catenin signaling is required for mutant *Kras*-driven acinar cell programming and is essential for PDAC carcinogenesis.[38] Consistent with this, nuclear translocation of β-catenin and activation of Wnt pathway target genes are observed in PanINs and PDAC.[39,40] We previously showed that PYK2 and FAK function redundantly to promote the Wnt/β-catenin pathway by phosphorylating glycogen synthase kinase 3α/3β (GSK3α/3β) at tyrosine 279 and tyrosine Y216, respectively, in colorectal cancer cells.[41] In PDAC cells, we found that knockdown of *PYK2* suppressed the messenger RNA levels of Wnt target genes

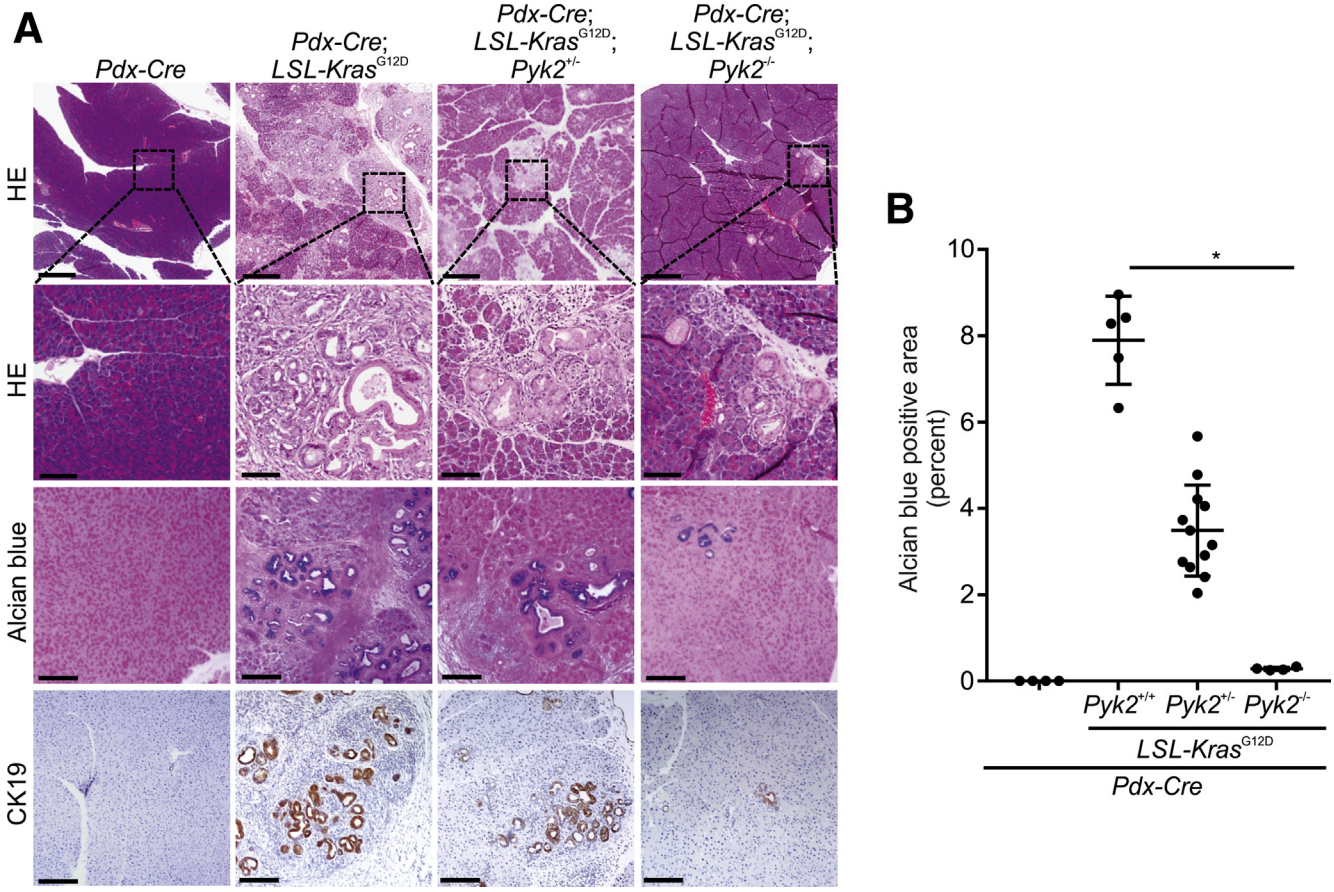

Figure 4. PYK2 is required for mutant *KRAS*-induced pancreatic carcinogenesis. (*A*) The pancreatic tissues from 5- to 6-month-old *Pdx-Cre*, *Pdx-Cre*;*LSL-Kras*^{G12D}, *Pdx-Cre*;*LSL-Kras*^{G12D};*Pyk2*$^{+/-}$, and *Pdx-Cre;LSL-Kras*^{G12D};*Pyk2*$^{-/-}$ mice were collected for H&E, Alcian blue/eosin, and anti-CK19 antibody staining. *Scale bars*: H&E (first row), 500 μm; (second row), 100 μm; Alcian blue/eosin, 200 μm; CK19, 200 μm. (*B*) Quantification of area positive for Alcian blue staining in pancreatic tissues from indicated genotypes. The number of mice in each group were as follows: *Pdx-Cre* (n = 4), *Pdx-Cre*;*LSL-Kras*^{G12D} (n = 5), *Pdx-Cre*;*LSL-Kras*^{G12D};*Pyk2*$^{+/-}$ (n = 12), and *Pdx-Cre*;*LSL-Kras*^{G12D};*Pyk2*$^{-/-}$ (n = 4). Data are presented as means ± SD. *$P <$ .05 (Student *t* test).

without affecting the phosphorylation status of GSK3α/3$\beta^{Y279/Y216}$ (Figure 7*B* and *C*). These results support the notion that PYK2 functions through phosphorylating β-catenin or other key Wnt/β-catenin pathway components.

β-catenin can be phosphorylated at Y142,[42] Y654,[43] Y489,[44] and Y86.[45] To determine whether PYK2 directly phosphorylates these sites, we performed an in vitro kinase assay using human recombinant β-catenin as substrate and human recombinant PYK2 as candidate kinase. The results showed that among the earlier-mentioned sites on β-catenin, PYK2 was able to phosphorylate Y654 (Figure 7*D*). FAK is the other member of the FAK family.[46] As a kinase control, FAK did not phosphorylate β-catenin^{Y654} in vitro (Figure 7*D*), thus validating that in vitro phosphorylation of β-catenin^{Y654} is kinase specific.

Phosphorylation of β-catenin^{Y654} is known to release β-catenin from the cadherin complex to promote its nuclear translocation, resulting in an increase in T-cell factor (TCF)/β-catenin–mediated transcriptional activity.[45] We then examined whether PYK2 promotes β-catenin nuclear translocation. The results of the immunofluorescence analysis and cell fractionation experiment showed that shRNA down-regulation of *PYK2* did suppress nuclear translocation of β-catenin in PDAC cells (Figure 7*E* and *F*).

We next examined whether increased levels of phosphorylated β-catenin^{Y654} could be detected in mouse PDAC and acute pancreatitis models. Similar to the expression patterns of PYK2 and p-PYK2^{Y402}, the level of phosphrylated b-catenin at tyrosine 654 (p-b-catenin^{Y654}) was increased significantly in pancreatic tissues from *Pdx-Cre*;*LSL-Kras*^{G12D} mice and cerulein-treated *C57BL/6* mice (Figure 7*G* and *H*), supporting that an increase of β-catenin^{Y654} phosphorylation is an early event in PDAC initiation and correlates with the activation of PYK2. Finally, consistent with earlier studies,[16,39,40] our IHC results showed that β-catenin levels, particular nuclear β-catenin, was increased in mouse PanIN lesions in *Pdx-Cre*;*Kras*^{G12D} mice (Figure 7*I*) and ADM lesions induced by cerulein treatment in control *C57BL/6* mice (Figure 7*J*). Deletion of *Pyk2* not only greatly inhibited PanIN and ADM formation, but also almost completely blocked nuclear β-catenin increase in *Pdx-Cre*;*Kras*^{G12D} mice and cerulein-treated *C57BL/6* mice (Figure 7*I* and *J*). In light

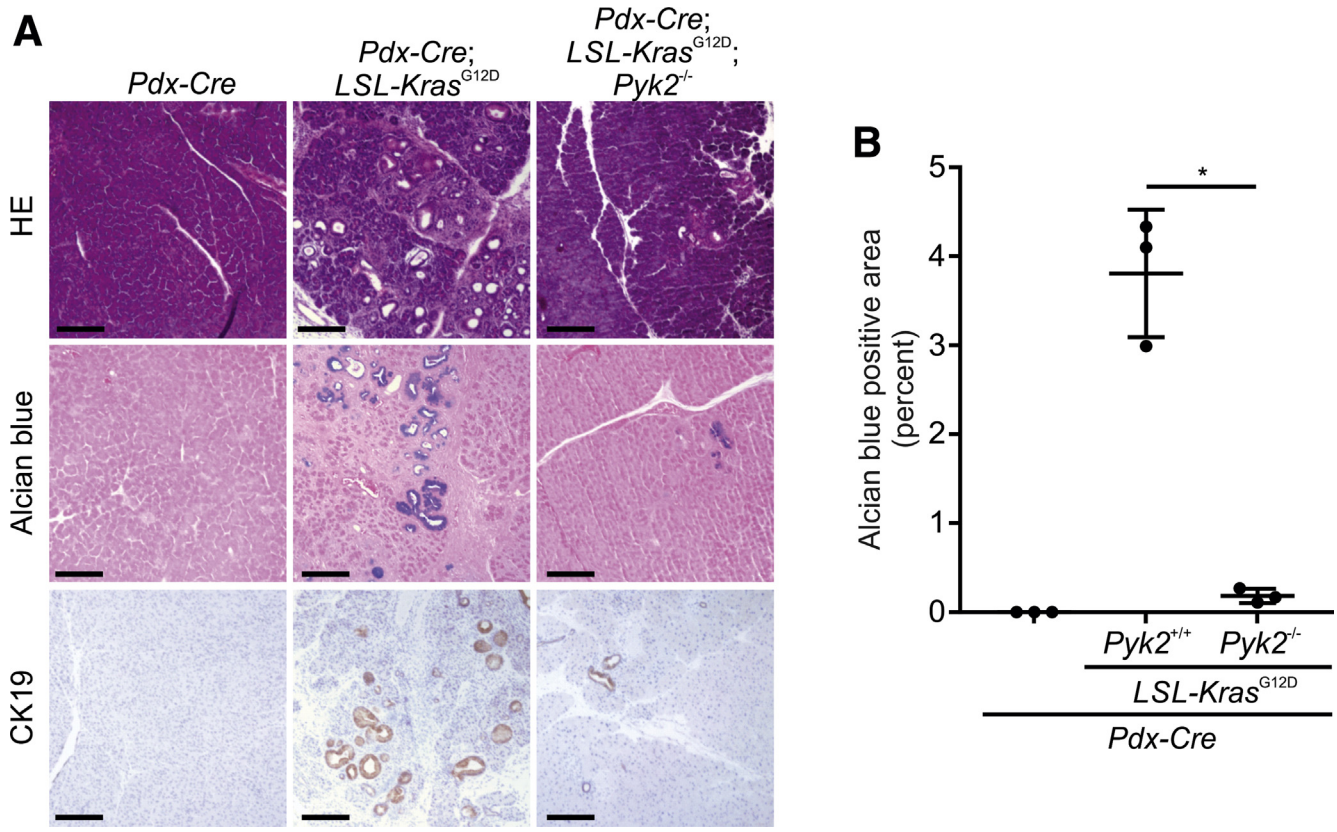

Figure 5. Mutant *Kras*-driven and pancreatitis-associated pancreatic tumorigenesis requires PYK2. (*A*) Six-week-old mice with indicated genotypes were treated with 1 set of cerulein injections for 2 consecutive days. Twenty days later, the pancreatic tissues were collected and processed for H&E, Alcian blue/eosin, and anti-CK19 antibody staining. *Scale bars*: 200 μm. (*B*) Quantification of Alcian blue–positive area in pancreatic tissues from indicated genotypes (n = 3). Data are presented as means ± SD. *$P < .05$ (Student *t* test).

of the finding that phosphorylation of β-catenin^{Y654} enhances Wnt signaling and promotes intestinal tumorigenesis in β-catenin^{Y654} knock-in mice,[47] our results strongly support the possibility that PYK2 is involved in PDAC initiation and development through phosphorylating β-catenin^{Y654} to promote Wnt/β-catenin pathway activation. Somatic mutations of the key components of the Wnt/β-catenin pathway are rare in PDAC.[48] Although ample evidence supports the involvement of Wnt/β-catenin signaling in PDAC tumorigenesis,[38–40] how the pathway is dysregulated in PDAC and how its activation contributes to PDAC remain to be determined. Our findings not only provide further support for the role of Wnt/β-catenin pathway activation in PDAC, but also offered new mechanistic insights on how the Wnt/β-catenin pathway is activated in PDAC. Finally, the results that knockdown of *STAT3* or *YAP/TAZ* in PDAC cells inhibited β-catenin phosphorylation at Y654 strongly supports the proposed YAP/TAZ/STAT3/PYK2/β-catenin signaling axis (Figure 7*K* and *L*).

PYK2 Is Required for In Vitro Cell Proliferation and Xenograft Growth of Human PDAC Cells

In addition to PDAC initiation and development, we also tested whether PYK2 plays a role in PDAC maintenance. The results from the cell proliferation assay showed that knockdown of *PYK2* by 2 specific shRNAs significantly suppressed PDAC cell proliferation, which can be partially restored by ectopic expression of *β-catenin*^{Y654E} (phosphormimetic mutant of *β-catenin*^{Y654}) in *PYK2* knockdown cells (Figure 8*A* and *B*). Furthermore, results of a xenograft tumor assay showed that knockdown of *PYK2* suppressed in vivo tumor growth of PDAC cells, whereas overexpression of *β-catenin*^{Y654E} substantially restored the tumor growth of *PYK2* knockdown cells in nude mice (Figure 8*C*). These findings indicated that PYK2 is required for PDAC maintenance and PYK2 exerts its function through phosphorylating β-catenin at Y654.

Discussion

There is significant interest in identifying novel cancer targets for PDAC prevention and treatment that could be amenable to pharmacologic intervention. The current study has identified PYK2 as such a target that is required for the induction of ADM, initiation of PanIN, and PDAC maintenance (Figure 8*D*). In this study, we show that PYK2 and p-PYK2^{Y402} are highly abundant in ADM and PanIN lesions, and the transcription of *PYK2* is regulated by YAP/TAZ and mediated by STAT3. These findings show a novel regulatory circuit in PDAC cells that involves YAP/TAZ/STAT3/PYK2.

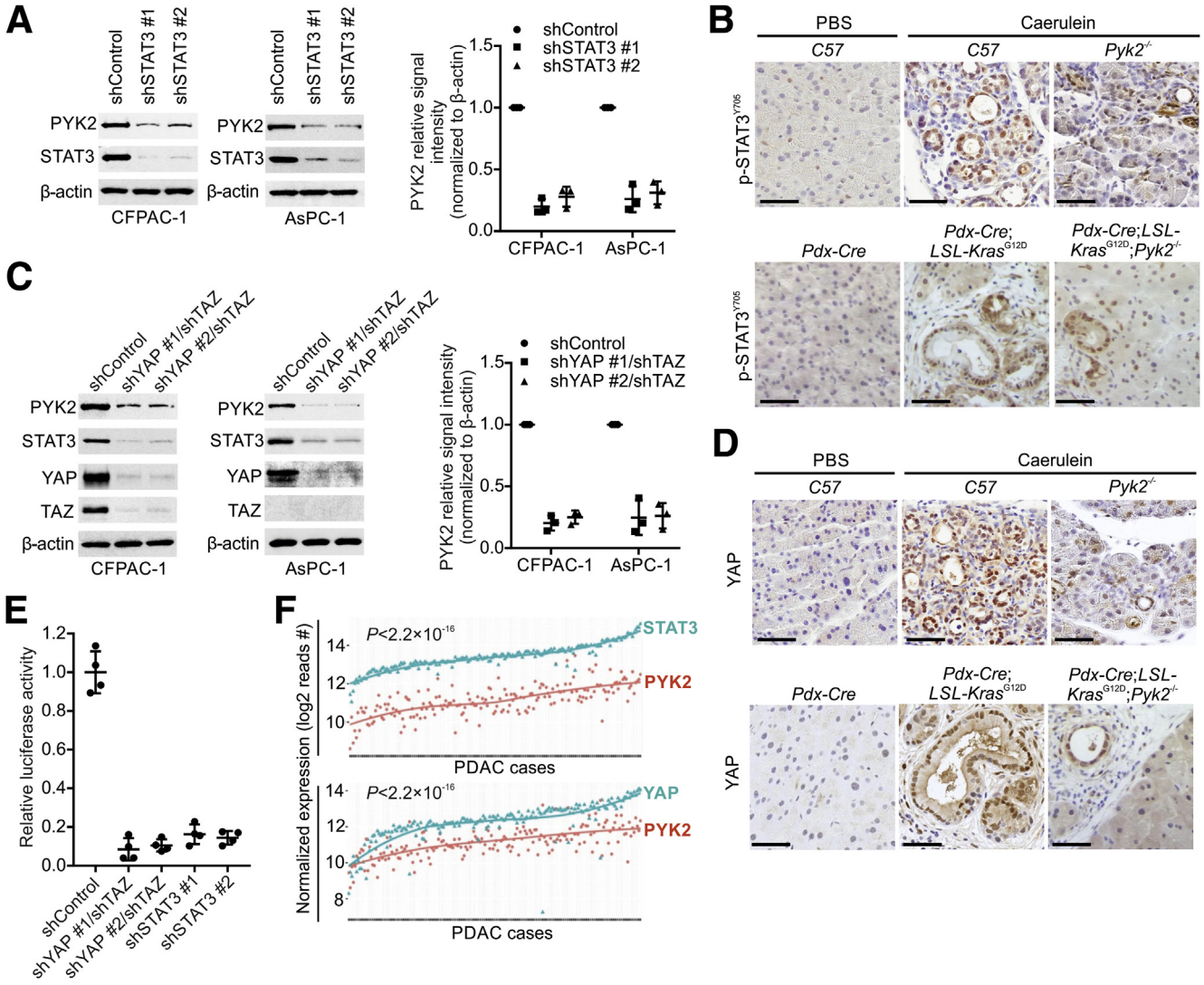

Figure 6. Gene transcription of *PYK2* in PDAC cells is YAP/TAZ- and STAT3-dependent. (*A*) *Left and middle*: the whole-cell lysates from CFPAC-1 and AsPC-1 scrambled shRNA control cells or *STAT3* shRNA knockdown cells were used for immunoblotting with indicated antibodies. *Right*: quantified immunoblotting data for PYK2 from 3 independent experiments are presented as means ± SD. (*B*) *Upper*: IHC staining of p-STAT3^{Y705} was performed in pancreatic tissue sections from 6-week-old indicated mice injected with 1 set of PBS or cerulein for 2 consecutive days. The pancreatic tissues were collected 2 days after injection. *Scale bars*: 50 μm. *Lower*: IHC staining of p-STAT3^{Y705} was performed in pancreatic tissue sections from 6-month-old indicated mice. *Scale bars*: 50 μm. Representative images from 3 independent experiments are shown. (*C*) *Left and middle*: Western blots were performed with indicated antibodies using the whole-cell lysates from CFPAC-1 and AsPC-1 scrambled shRNA control cells and *YAP/TAZ* double-knockdown cells. TAZ level was barely detected in AsPC-1 cells. *Right*: quantified immunoblotting data for PYK2 from 3 independent experiments are presented as means ± SD. (*D*) IHC staining of YAP was performed on consecutive sections described in panel *B*. *Scale bars*: 50 μm. Representative images from 3 independent experiments are shown. (*E*) pGL3 vector encompassing *PYK2* promoter region (from -2063 bp to +113 bp) was co-transfected with pRL-TK into CFPAC-1 scrambled shRNA control cells or indicated shRNA knockdown cells. Forty-eight hours after transfection, the cells were collected for luciferase assays using the dual-luciferase reporter assay system. The data are presented as fold changes to shRNA control and are representative of 3 independent experiments. Values are means ± SD. (*F*) Co-expression of *YAP*, *STAT3*, and *PYK2* in PDAC cases from the TCGA database. *P* values were determined using a paired Student *t* test.

Furthermore, we have identified β-catenin as a downstream target for PYK2 kinase activity. Our data indicate that PYK2 is involved in PDAC initiation, development, and maintenance by activating the Wnt/β-catenin pathway. PDAC frequently is associated with deregulation of crucial cancer-related signaling pathways including the Hippo signaling pathway (via its downstream effector YAP and TAZ),[32–34] STAT3 signaling,[28–30] and the Wnt/β-catenin pathways.[38] Mechanistically, how each one of these pathways is activated or how it interacts in pancreatic carcinogenesis remains to be determined. The current study identified PYK2 as a novel signaling node connecting these key pathways in PDAC, thus adding important molecular insights into PDAC biology.

PDAC remains one of the most devastating human diseases because of limited treatment options. The 2016 report that single-agent treatment with the dual FAK/PYK2 inhibitor VS-4718 or combined treatment with VS-4718 and programmed cell death-1 (PD-1) inhibitor elicited significant tumor regression in the *p48-Cre*;*LSL-Kras*^{G12D};*p53*$^{flox/+}$ (KPC) mouse model[21] has brought excitement to the field of PDAC. However, the results of a recent phase II trial of GSK2256098 (FAK-specific inhibitor) and trametinib (mitogen-activated protein kinase kinase [MEK1/2] inhibitor) in patients with advanced PDAC (MOBILITY-002 Trial, NCT02428270) showed that GSK2256098 and trametinib were not active in unselected advanced PDAC,[49] suggesting that FAK inhibition alone is not sufficient to exert a therapeutic effect in PDAC patients. The current study provides genetic evidence for the essential role of PYK2 in PDAC genesis and maintenance. Our findings indicate that PYK2 plays a cell-autonomous role in PDAC cells. That said, we believe that effective FAK inhibition as well as PYK2 inhibition may lead to better treatment outcomes in PDAC patients.

PYK2 and FAK are related structurally and they can function redundantly and nonredundantly in a function- and context-dependent manner.[50] In adult mice, endothelial cell–specific FAK inactivation is associated with increased PYK2 expression that enables growth factor–stimulated angiogenesis in the absence of FAK.[51] Increased PYK2 expression also occurs in vitro upon FAK inactivation in primary fibroblasts and endothelial cells.[51,52] The current study indicates that FAK or other tyrosine kinases do not compensate for PYK2 loss in mutant KRAS-induced PDAC initiation and development, implying that PYK2 and FAK do not function redundantly in PDAC carcinogenesis.

Similar to PYK2, FAK also is hyperactivated in neoplastic PDAC cells.[21] Dual FAK/PYK2 inhibition rendered the previously unresponsive KPC mouse model responsive to T-cell immunotherapy and PD-1 antagonists,[21] supporting that FAK is an important regulator of the fibrotic and immunosuppressive tumor microenvironment. Because PYK2 has been shown to be important in wound healing and myeloid cell migration and differentiation,[20,53,54] it is highly possible that PYK2 also plays a critical role in driving the fibrotic and immunosuppressive tumor microenvironment in PDAC. Further studies are needed to dissect the impact of tumor cell–intrinsic PYK2 on cancer cells and stromal cells of the tumor microenvironment, including endothelial cells, fibroblasts, and leukocytes.

In summary, the current study has identified a critical role for PYK2 in acinar-to-ductal metaplasia reprogramming en route to pancreatic carcinogenesis and in PDAC maintenance. PYK2 activation in this context requires a YAP/TAZ/STAT3 signaling axis and results in activation of the Wnt/β-catenin pathway. The important role of PYK2 in the formation of metaplastic ducts in pancreatitis suggests that targeting PYK2 could restore homeostasis and reduce the chance of tumorigenesis in at-risk patients. The requirement of PYK2 in PDAC maintenance suggests that PYK2 can serve as a promising therapeutic target for PDAC. Given that PYK2 expression is tissue- and cell type–restricted, and that PYK2 increases occur predominantly in pancreatic lesions and PDAC tumor tissues, targeting PYK2 activation could be an important and safe approach to the prevention and treatment of PDAC.

Methods

Mice

All animal procedures were performed according to protocols approved by the Institutional Animal Care and Use Committee at the University of Pittsburgh. Mice were fed a standard diet (diet ID 5P75; Purina LabDiet, St. Louis, MO). *Pyk2* knockout mice[20] were obtained from Pfizer (New York, NY) through Dr Tatiana Efimova (Washington University in St. Louis, St. Louis, MO), and maintained on a *C57BL/6* background. Genotyping was performed as previously described.[55] The following primers were used: 5'-CCTGCTGGCAGCCTAACCACAT-3' (common reverse primer), 5'-GGAGGTCTATGAAGGTGTCTACACGAAC-3' (wild-type forward primer) and 5'-GCCAGCTCATTCCTCCCACTCAT-3' (knockout forward primer). Polymerase chain reaction (PCR) conditions were as follows: denature at 95°C for 5 minutes; then 40 cycles of 94°C for 45 seconds, 62°C for 45 seconds, and 72°C for 1 minute; and then held at 72°C for 5 minutes before cooling to 4°C. *Pdx-Cre* and *LSL-Kras*^{G12D} mice were received from the NCI Mouse Repository (Frederick, MD), and crossed with *C57BL/6* to maintain on a mixed background. These mice were crossed to generate indicated animals.

For xenograft experiments, 3×10^6 CFPAC-1 cells were injected subcutaneously into both flanks of 4- to 5-week-old athymic nude mice (Charles River Laboratories, Wilmington, MA), 5 mice in each group. The mice were housed in a sterile environment. Tumor size was determined by caliper measurements twice a week. The tumor volume was calculated using the following formula: $V = {}^1/_2 \times a \times b^2$, where a and b denoted the largest and smallest tumor axis, respectively.

Explant Culture of Mouse Acinar Cells

Primary acinar cells were isolated from mice and cultured as previously described.[25] Briefly, a 24-well cell culture plate was coated with a 200-μL layer of collagen gel mixture containing 180 μL of rat tail collagen (Thermo Fisher Scientific, Waltham, MA), 20 μL of unsupplemented 10$\times$ Waymouth medium (Sigma-Aldrich, St. Louis, MO), and 0.8 μL of 5 N NaOH. After the four-week-old mice were euthanized, the pancreas was dissected out immediately, rinsed twice with ice-cold Hank's balanced salt solution (HBSS), minced into small pieces, and digested with 0.2 mg/mL collagenase P (Sigma-Aldrich; St. Louis, MO) in HBSS for 15 minutes at 37°C with gentle shaking. The digestion was stopped by adding ice-cold HBSS with 5% fetal bovine serum (FBS). The cells then were washed 3 times with HBSS with 5% FBS and subsequently pipetted through 500-μm and 105-μm polypropylene mesh (Spectrum Laboratories, Rancho Dominguez, CA). The cell suspension was carefully added to the top of the HBSS with 30% FBS and centrifuged

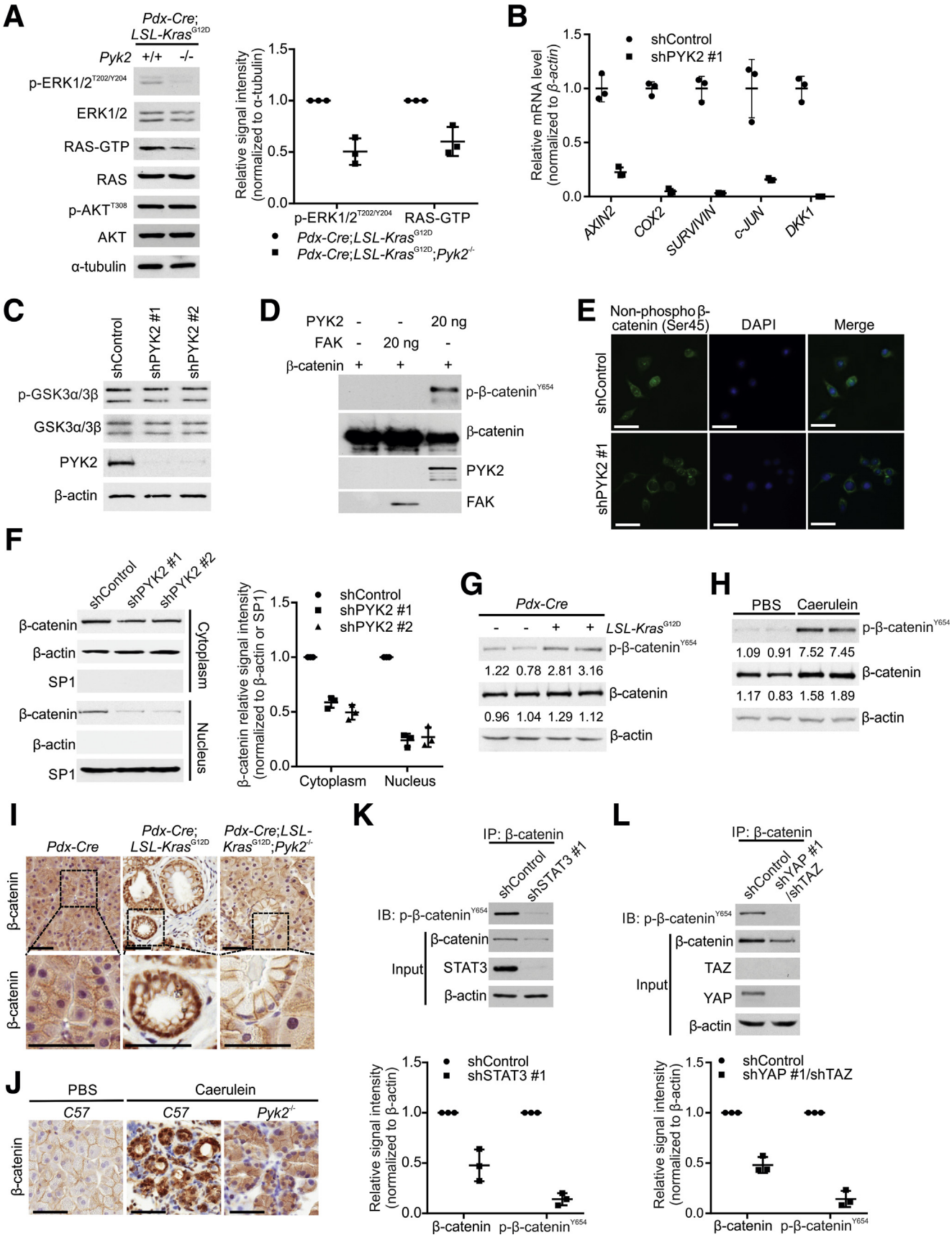
A
Pdx-Cre; LSL-Kras^G12D
Pyk2 +/+ -/-
p-ERK1/2^T202/Y204
ERK1/2
RAS-GTP
RAS
p-AKT^T308
AKT
α-tubulin
Relative signal intensity (normalized to α-tubulin)
p-ERK1/2^T202/Y204
RAS-GTP
Pdx-Cre;LSL-Kras^G12D
Pdx-Cre;LSL-Kras^G12D;Pyk2^-/-
B
shControl
shPYK2 #1
Relative mRNA level (normalized to β-actin)
AXIN2
COX2
SURVIVIN
c-JUN
DKK1
C
shControl
shPYK2 #1
shPYK2 #2
p-GSK3α/3β
GSK3α/3β
PYK2
β-actin
D
PYK2 - - 20 ng
FAK - 20 ng -
β-catenin + + +
p-β-catenin^Y654
β-catenin
PYK2
FAK
E
Non-phospho β-catenin (Ser45)
DAPI
Merge
shControl
shPYK2 #1
F
shControl
shPYK2 #1
shPYK2 #2
β-catenin
β-actin
SP1
Cytoplasm
Nucleus
β-catenin relative signal intensity (normalized to β-actin or SP1)
Cytoplasm
Nucleus
G
Pdx-Cre
LSL-Kras^G12D
p-β-catenin^Y654
1.22 0.78 2.81 3.16
β-catenin
0.96 1.04 1.29 1.12
β-actin
H
PBS
Caerulein
p-β-catenin^Y654
1.09 0.91 7.52 7.45
β-catenin
1.17 0.83 1.58 1.89
β-actin
I
Pdx-Cre
Pdx-Cre; LSL-Kras^G12D
Pdx-Cre;LSL-Kras^G12D;Pyk2^-/-
β-catenin
β-catenin
J
PBS
Caerulein
C57
C57
Pyk2^-/-
β-catenin
K
IP: β-catenin
shControl
shSTAT3 #1
IB: p-β-catenin^Y654
Input
β-catenin
STAT3
β-actin
Relative signal intensity (normalized to β-actin)
shControl
shSTAT3 #1
β-catenin
p-β-catenin^Y654
L
IP: β-catenin
shControl
shYAP #1 /shTAZ
IB: p-β-catenin^Y654
Input
β-catenin
TAZ
YAP
β-actin
Relative signal intensity (normalized to β-actin)
shControl
shYAP #1/shTAZ
β-catenin
p-β-catenin^Y654

at 180*g* for 2 minutes at 4°C. The cell pellet was resuspended in cold Waymouth medium containing 10% FBS, 1% penicillin/streptomycin, 100 μg/mL trypsin inhibitor (Sigma-Aldrich), and 1 μg/mL of dexamethasone (Sigma-Aldrich). An equal volume of cell suspension was mixed with collagen gel mixture and 500 μL of the mixture was added into each well of the precoated 24-well plate. After the cell/collagen mixture solidified, complete Waymouth medium was pipetted carefully onto the top of the mixture. To achieve Cre-mediated activation of the mutant *Kras* allele, acinar cells were infected with adenoviruses expressing Cre recombinase or green fluorescent protein (GFP) (SignaGen Laboratories, Rockville, MD) at a concentration of 1.5×10^7 plaque-forming U/mL for 1 hour at 37°C before suspending the epithelium in the collagen gel mixture. To study TGF-α–induced ADM transition, the acinar cells were maintained with or without 50 ng/mL recombinant TGF-α (Abcam, Cambridge, MA). The acinar cells were cultured in a 37°C humidified incubator containing 5% CO_2. Medium was changed on day 1 and day 3 after plating. Pictures were taken on day 5. To prepare the explants for immunofluorescence staining, the whole collagen gels were fixed in 10% neutral buffered formalin and processed as described in the *Immunohistochemistry and Immunofluorescence Staining* section.

Cell Lines

All cells were obtained from American Type Culture Collection (Manassas, VA) and cultured in a 37°C humidified incubator containing 5% CO_2. AsPC-1 cells and CFPAC-1 cells were grown in RPMI-1640 medium and Dulbecco's modified Eagle medium, respectively. All cells were supplemented with 5% FBS, 100 U/mL penicillin, and 100 μg/mL streptomycin.

Transient Transfection, Lentivirus Production, and Infection

Plasmid transient transfections were performed using PolyJet In Vitro DNA Transfection Reagent (SignaGen Laboratories) according to the manufacturer's instructions. Lentiviruses encoding shRNA for specific genes were produced in human embryonic kidney (HEK) 293T cells by transfection of the lentiviral vector expressing shRNA with the third-generation packaging systems (Addgene, Cambridge, MA). The media containing viral particles were filtered through syringe filters and subsequently used to infect target cells. Cell lines stably expressing shRNA were established by antibiotic selection. Cells expressing scrambled shRNA (Addgene) were used as shRNA control. G418 and puromycin were combined to select the cells stably expressing *β-catenin*^{Y654E} and *PYK2* shRNA.

Immunoprecipitation, Immunoblotting, and RAS Activity Assay

The immunoprecipitation was performed as previously described.[41] Whole-cell lysates were prepared in lysis buffer (20 mmol/L Tris-HCl, pH 7.5, 150 mmol/L NaCl, 1 mmol/L EDTA, 1% NP40, and 10% glycerol) supplemented with protease inhibitor and phosphatase inhibitor (Thermo Fisher Scientific), resolved by sodium dodecyl sulfate–polyacrylamide gel electrophoresis (SDS-PAGE), and blotted with the antibodies indicated in figures. SuperSignal West Pico Chemiluminescent Substrate and SuperSignal Western Blot Enhancer (Thermo Fisher Scientific) were used to enhance blotting signal when needed. RIPA buffer

Figure 7. (***See previous page***). **PYK2 activates the Wnt/β-catenin pathway through phosphorylating β-catenin^{Y654}.** (*A*) Deletion of PYK2 affects ERK1/2 and RAS activity. Pancreatic tissue lysates from indicated mice (age, 4 mo) were used for immunoblotting with the indicated antibodies. To detect Guanosine-5'-triphosphate (GTP)-bound RAS, the lysates were incubated with rapidly accelerated fibrosarcoma (RAF) RAS binding domain (RBD) agarose. The bound proteins then were resolved by SDS-PAGE and blotted with anti-RAS antibody. Quantified immunoblotting data from 3 independent experiments are presented as means ± SD. (*B*) Messenger RNA (mRNA) from AsPC-1 scrambled shRNA control cells and *PYK2* knockdown cells was isolated for quantitative reverse-transcription PCR. *β-actin* was used as an internal control. The data are presented as fold change to shRNA control in triplicate and are representative of 3 independent experiments. Values are means ± SD. (*C*) Lysates from scrambled shRNA control AsPC-1 cells and *PYK2* knockdown cells were used for immunoblotting with the indicated antibodies. The representative result of 3 independent experiments is shown. (*D*) Recombinant β-catenin (100 ng) was incubated with purified PYK2 or FAK recombinant protein (or kinase buffer as a negative control) in the presence of adenosine triphosphate at 37°C for 1 hour. The reaction mixtures were subjected to immunoblotting analysis using the indicated antibodies. The representative result of 4 independent experiments is shown. (*E*) β-catenin localization was assessed in AsPC-1 scrambled shRNA cells and *PYK2* knockdown cells using immunofluorescence staining. *Scale bars*: 50 μm. Representative images of 3 independent experiments are shown. (*F*) Cytoplasmic and nuclear fractions of scrambled shRNA control AsPC-1 cells and *PYK2* knockdown cells were used for immunoblotting with the indicated antibodies. Quantified immunoblotting data from 3 independent experiments are presented as means ± SD. (*G*) Immunoblotting analysis was performed using pancreatic tissue lysates from 4-month-old *Pdx-Cre* mice and *Pdx-Cre*;*LSL-Kras*^{G12D} mice. Each lane represents a single mouse. (*H*) Six-week-old *C57BL/6* mice were injected with cerulein or PBS for 2 consecutive days. The pancreatic tissues were collected 2 days after injection for immunoblotting analysis with the indicated antibodies. (*G* and *H*) Representative immunoblotting results from 3 independent experiments are shown. The numbers under each blot represent the band intensity normalized to β-actin and relative to expression of target proteins in *Pdx-Cre* mice or PBS-treated *C57BL/6* mice. (*I*) IHC staining of β-catenin in pancreatic sections from indicated mice. *Scale bars*: 50 μm. (*J*) Six-week-old indicated mice were injected with cerulein or PBS for 2 consecutive days. The pancreatic tissues were collected 2 days after the last injection and processed for IHC staining with anti–β-catenin antibody. *Scale bars*: 50 μm. Representative images of 3 independent experiments are shown. (*K* and *L*) The whole-cell lysates from AsPC-1 scrambled shRNA control cells or cells with indicated gene knockdown were used for immunoprecipitation or immunoblotting with the indicated antibodies. Quantified immunoblotting data from 3 independent experiments are presented as means ± SD. DAPI, 4′,6-diamidino-2-phenylindole.

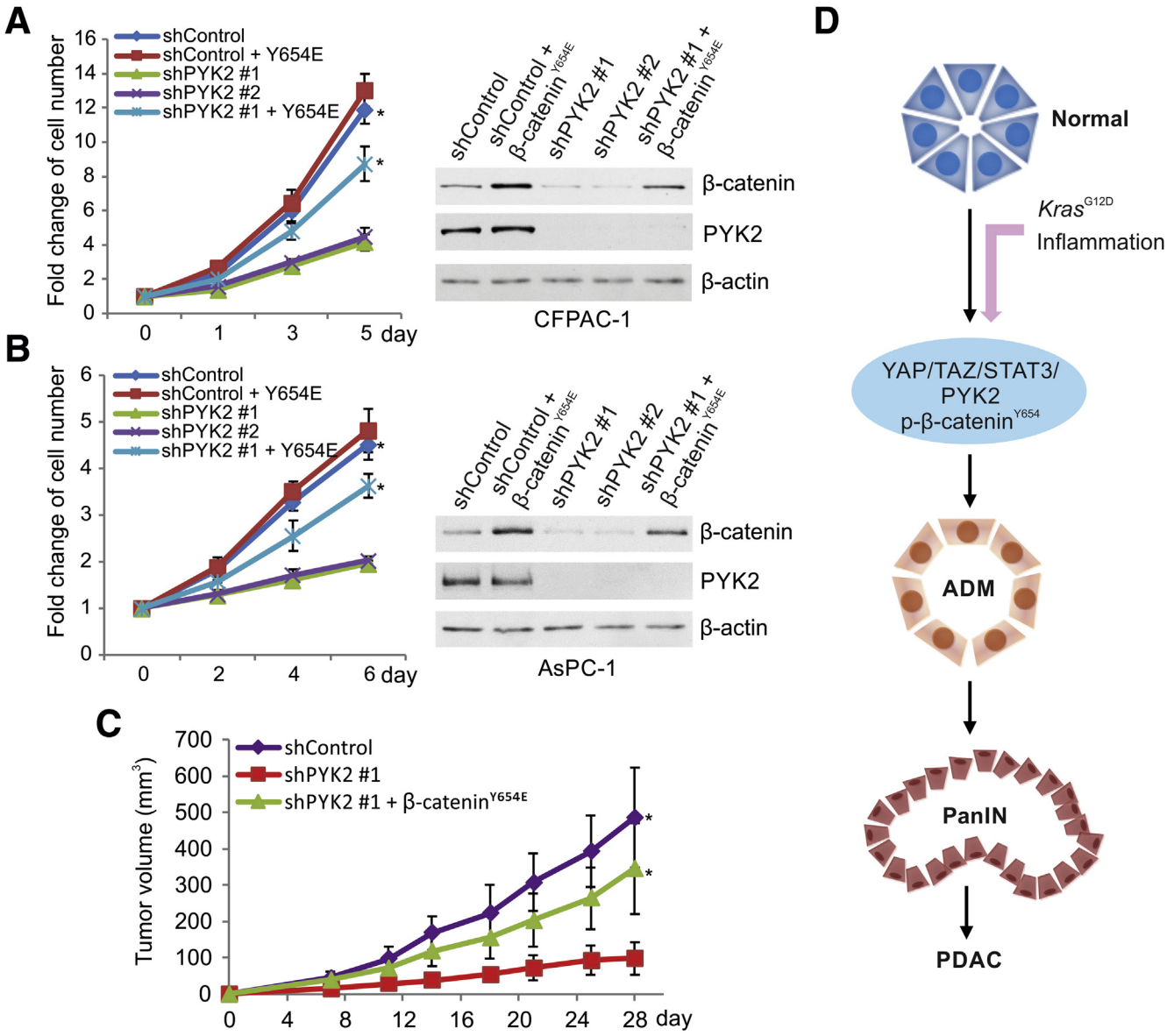

Figure 8. PYK2 promotes PDAC cell proliferation and in vivo tumor growth by phosphorylating β-catenin^{Y654}. (*A* and *B*) *Left*: cell viability of the indicated cell lines was determined by cell counting kit-8 (CCK-8) assay. Data are presented as means ± SD from 3 independent experiments. *Statistically significant difference ($P < .05$, Student *t* test) when compared with cells expressing *PYK2* shRNA 1. *Right*: immunoblotting analysis of cell lines used in the cell viability assay with the indicated antibodies. (*C*) Indicated CFPAC-1 cells were injected into both flanks of nude mice (5 mice in each cell group). Tumor sizes were measured at the indicated time points. Tumor volumes were calculated and plotted. Values are means ± SD. *Statistically significant difference ($P < .05$, Student *t* test) when compared with the *PYK2* knockdown group. (*D*) Schematic diagram summarizing the YAP/TAZ/STAT3/PYK2/p–β-catenin^{Y654} axis in PDAC initiation.

(Thermo Fisher Scientific) supplemented with protease inhibitor and phosphatase inhibitor was used to extract protein from mouse pancreatic tissue. NE-PER Nuclear and Cytoplasmic Extraction Reagents from Thermo Fisher Scientific were used for subcellular fractionation according to the manufacturer's protocol. RAS activity was determined by the RAS activation assay kit (Millipore, Burlington, MA) using rapidly accelerated fibrosarcoma (RAF) RAS binding domain (RBD) agarose beads according to the manufacturer's protocol. The precipitates were subjected to SDS-PAGE and immunoblotted with anti-RAS antibody. Signal intensities of Western blot bands were quantified using ImageJ software (National Institutes of Health, Bethesda, MD). The antibodies used in immunoblotting are listed in Table 1.

Plasmids

Lentiviral-based shRNA plasmids for targeting *PYK2*, *YAP*, and *STAT3* were purchased from Sigma-Aldrich: *PYK2* shRNA 1, TRCN0000199334; *PYK2* shRNA 2, TRCN0000199771; *YAP* shRNA 1, TRCN0000107266; *YAP* shRNA 2, TRCN0000107267; *STAT3* shRNA 1, TRCN0000329887; *STAT3* shRNA 2, TRCN0000329888. To construct lentiviral-based

Table 1. Antibody Used in This Study

Name	Company	Catalog number	Dilution
α-tubulin	Cell Signaling Technology	3873	1:2000 (IB)
β-actin	Santa Cruz Biotechnology (Dallas, TX)	sc-81178	1:2000 (IB)
PYK2	Cell Signaling Technology	3090	1:1000 (IB)
PYK2	Santa Cruz Biotechnology	sc-1515	1:25 (IHC)
p-PYK2^{Y402}	Thermo Fisher Scientific	44-618G	1:50 (IF, IHC); 1:500 (IB)
YAP	Cell Signaling Technology	4912	1:1000 (IB)
YAP	Cell Signaling Technology	14074	1:200 (IHC)
TAZ	R&D systems (Minneapolis, MN)	MAB7210-SP	1:750 (IB)
STAT3	Cell Signaling Technology	4904	1:1000 (IB)
p-STAT3^{Y705}	Cell Signaling Technology	9145	1:50 (IHC)
CK19	DSHB (University of Iowa)	TROMA-III	1:25 (IF, IHC)
p–β-catenin^{Y654}	Abcam	ab59430	1:400 (IB)
FAK	Cell Signaling Technology	3285	1:1000 (IB)
β-catenin	Cell Signaling Technology	9582	1:50 (IHC) 1:1000 (IB)
β-catenin	BD Biosciences (San Jose, CA)	610153	1:2000 (IB); 1:50 (IP)
Nonphospho–β-catenin (Ser45)	Cell Signaling Technology	19807	1:500 (IF)
ERK1/2	Cell Signaling Technology	9102	1:1000 (IB)
p-ERK1/2	Cell Signaling Technology	4370	1:1000 (IB)
p-AKT^{T308}	Cell Signaling Technology	13038	1:1000 (IB)
AKT	Cell Signaling Technology	9272	1:1000 (IB)
RAS	Cell Signaling Technology	8955	1:1000 (IB)
GSK3α/3β	Santa Cruz Biotechnology	Sc-7291	1:1000 (IB)
p-GSK3α/3$\beta^{Y279/Y216}$	Santa Cruz Biotechnology	Sc-135653	1:1000 (IB)
Specificity protein 1 (SP1)	Santa Cruz Biotechnology	Sc-14027	1:1000 (IB)

IB, immunoblotting; IF, immunofluorescence.

vectors for TAZ knockdown, primers containing the sequence of shRNA oligonucleotides for *TAZ* (5′-CCAGGAA CAAACGTTGACTTA-3′) were annealed and ligated into pLKO.1-blasticidin, which was obtained from Addgene. The promoter region of the human *PYK2* gene, which encompassed the sequence from 2063 base pairs upstream of the transcription start codon to 113 base pairs downstream of the transcription start codon, was amplified by PCR and subsequently cloned into pGL3-Basic vector (Promega, Madison, WI). *β-catenin* phosphorylation mutant was generated by PCR-directed mutagenesis using pcDNA3–β-catenin (Addgene) as template.

In Vitro Kinase Assay

The in vitro assay to assess kinase activity of PYK2 toward β-catenin was performed in a total volume of 15 μL at 37°C for 1 hour. The components were as follows: 20 ng full-length recombinant PYK2 (Enzo, Farmingdale, NY), 2 mmol/L adenosine triphosphate (Cell Signaling Technology, Danvers, MA), kinase buffer (Cell Signaling Technology), and 100 ng full-length recombinant β-catenin (Abcam). The reaction with 20-ng full-length recombinant FAK (SignalChem, British Columbia, Canada) as kinase was set up as a control. The reaction product was subjected to SDS-PAGE followed by immunoblotting with antibody recognizing p–β-catenin^{Y654}.

RNA Extraction and Quantitative Reverse-Transcription PCR Analysis

Total RNA was extracted from cells using the RNeasy Mini Kit (Qiagen, Germantown, MD). The DNase-treated RNA was reverse-transcribed using SuperScript III reverse transcriptase (Invitrogen, Carlsbad, CA). The PCR reactions were performed using SYBR Select Master Mix (Thermo Fisher Scientific). The following primers were used: *AXIN2*, 5′-CAAGGGCCAGGTCAC-CAA-3′ (forward) and 5′-CCCCCAACCCATCTTCGT-3′ (reverse); *COX2*, 5′-CCCTTGGGTGTCAAAGGTAA-3′ (forward) and 5′-GCCCTCGCTTATGATCTGTC-3′ (reverse); *SURVIVIN*, 5′-TCCACTGCCCCACTGAGAAC-3′ (forward) and 5′-TGGCTCC CAGCCTTCCA-3′ (reverse); *c-JUN*, 5′-ATCAAGGCG GAGAGGAAGCG-3′ (forward) and 5′-TGAGCATGTTGGCCG TGGAC-3′ (reverse); *DKK1*, 5′-CTCGGTTCTCAATTCCAACG-3′ (forward) and 5′-GCACTCCTCGTCCTCTG-3′ (reverse); *β-actin*, 5′-TTGTTACAGGAAGTCCCTTGCC-3′ (forward) and 5′-ATGC-TATCACCTCCCCTGTGTG-3′ (reverse).

Acute Pancreatitis Induction

Mouse acute pancreatitis was induced by 6 hourly intraperitoneal injections of cerulein (Sigma-Aldrich) dissolved in phosphate-buffered saline (PBS) on 2 consecutive days at a dose of 50 μg/kg. The control mice were given saline with the same injection regimen.

Immunohistochemistry and Immunofluorescence Staining

Formalin-fixed and paraffin-embedded tissue microarrays of human PDAC tissue microarrays were purchased from US Biomax, Inc (Derwood, MD). The mouse pancreas was dissected out, fixed overnight in 10% neutral buffered formalin, embedded in paraffin, and finally cut into 5-μm sections. The sections were deparaffinized in xylene solutions and rehydrated in graded alcohol solutions followed by washes in distilled water. Antigen retrieval was performed for 10 minutes in boiling 10 mmol/L sodium citrate (pH 6) solution with 1 mmol/L EDTA. The sections were allowed to cool to room temperature and then washed with PBS. The endogenous peroxidase was blocked with 3% hydrogen peroxide for 10 minutes. After washing with PBS, the sections were blocked with 20% goat serum diluted in PBS for 30 minutes. Sections then were incubated overnight at 4°C in a humidified chamber with primary antibodies diluted in 10% goat serum. The antibodies used in tissue staining are listed in Table 1.

For immunohistochemistry, the sections were washed with PBS and incubated with biotin-conjugated secondary antibodies diluted in 5% goat serum for 1 hour at room temperature. Then, the sections were washed again with phosphate buffered saline with tween-20 (PBST) and incubated with Vectastain Elite ABC reagents (Vector Laboratories, Burlingame, CA) for 30 minutes at room temperature. Color visualization was performed with 3.3'-diaminobenzidine until the brown color fully developed. The sections were counterstained with hematoxylin, dehydrated, and coverslippped with permanent mounting media. For immunohistochemistry with anti–β-catenin antibody, the procedures were modified slightly, as follows: (1) antigen retrieval was performed for 30 minutes in 10 mmol/L sodium citrate (pH 6) solution supplemented with 1 mmol/L EDTA and 0.05% Tween-20; (2) all wash steps were performed with phosphate buffered saline with tween-20 (PBST) buffer; and (3) primary antibody incubation was performed at room temperature for 2 hours.

For immunofluorescence, the sections were washed with PBS after primary antibody incubation and then incubated with secondary antibodies for 1 hour at room temperature. Finally the sections were washed with phosphate buffered saline with tween-20 (PBST) and counterstained with VectaShield plus 4′,6-diamidino-2-phenylindole (Vector Laboratories).

The images were acquired using an Olympus BX51 system microscope (Center Valley, PA) and processed using SPOT Advanced 5.1 software (SPOT Imaging, Sterling Heights, MI). For Alcian blue–positive area quantifications, 3 slides evenly distributed throughout the pancreas of each mouse were scanned using the Aperio digital pathology slide scanner (Leica Biosystems, Nussloch, Germany). The images were analyzed using Aperio ImageScope software. For ADM quantifications, the area containing ADM-like structures and eosin-positive areas were measured in 5 random fields of view from each H&E-stained section. Three sections for each mouse were analyzed. The percentage of ADM area was calculated by dividing the ADM-like lesion area by the total eosin-positive epithelial area. The ADM-like structures were determined according to the criteria described previously.[15]

Alcian Blue Staining

The sections were deparaffinized and hydrated to distilled water. Then the sections were immersed in 1% Alcian blue solution prepared in 3% acetic acid (pH 2.5) for up to 1 hour at room temperature. After washing with water, the slides were stained with eosin, dehydrated, and coverslippped with mounting media.

Immunocytochemistry

The cells were seeded in the 2-well chamber slide system (Cole-Parmer, Vernon Hills, IL) 1 day before the experiment. The cells were rinsed with PBS 3 times, fixed with prechilled methanol at room temperature for 5 minutes, and washed again with ice-cold PBS 3 times. Then the cells were incubated with 0.1% Triton X-100 (Sigma-Aldrich) in PBS for 5 minutes. The following procedures including epitope blocking and primary antibody and secondary antibody incubation were performed as described for immunofluorescence staining.

Luciferase Assay

Cells were seeded onto a 24-well plate 1 day before transfection. Luciferase reporter vector containing the *PYK2* promoter region was co-transfected with the thymidine kinase promoter-Renilla luciferase reporter plasmid (pRL-TK) into the cells. Forty-eight hours after transfection, the luciferase assays were performed using the dual-luciferase reporter assay system (Promega) according to the manufacturer's instructions. Renilla luciferase activity was used as an internal control to normalize the firefly luciferase activity.

Cell Proliferation Assays

AsPC-1 cells and CFPAC-1 cells were seeded onto 96-well plates at a density of 5×10^3 and 3×10^3, respectively. The cell viability was measured by cell counting kit-8 (CCK-8) (Sigma-Aldrich) according to the manufacturer's protocol at the indicated times.

Bioinformatics

R/bioconductor software was used in RNA sequencing analysis. The RNA sequencing data for PDAC were downloaded from the NCI's Genomic Data Commons and normalized using the TCGAbiolinks package. The log2 read counts then were presented by the ggplot2 package.

Statistical Analysis

Data are presented as means ± SD. The difference between the 2 groups was evaluated using the Student *t* test (2-tailed, unpaired). To study the expression association for the indicated genes based on TCGA data, a paired Student *t* test was used. *P* values less than .05 were considered statistically significant.

All authors had access to the study data and reviewed and approved the final manuscript.

References

1. Hruban RH, Adsay NV, Albores-Saavedra J, Compton C, Garrett ES, Goodman SN, Kern SE, Klimstra DS, Kloppel G, Longnecker DS, Luttges J, Offerhaus GJ. Pancreatic intraepithelial neoplasia: a new nomenclature and classification system for pancreatic duct lesions. Am J Surg Pathol 2001;25:579–586.
2. Guerra C, Mijimolle N, Dhawahir A, Dubus P, Barradas M, Serrano M, Campuzano V, Barbacid M. Tumor induction by an endogenous K-ras oncogene is highly dependent on cellular context. Cancer Cell 2003;4:111–120.
3. Zhu L, Shi G, Schmidt CM, Hruban RH, Konieczny SF. Acinar cells contribute to the molecular heterogeneity of pancreatic intraepithelial neoplasia. Am J Pathol 2007; 171:263–273.
4. De La OJ, Emerson LL, Goodman JL, Froebe SC, Illum BE, Curtis AB, Murtaugh LC. Notch and Kras reprogram pancreatic acinar cells to ductal intraepithelial neoplasia. Proc Natl Acad Sci U S A 2008; 105:18907–18912.
5. Eser S, Schnieke A, Schneider G, Saur D. Oncogenic KRAS signalling in pancreatic cancer. Br J Cancer 2014; 111:817–822.
6. Guerra C, Schuhmacher AJ, Canamero M, Grippo PJ, Verdaguer L, Perez-Gallego L, Dubus P, Sandgren EP, Barbacid M. Chronic pancreatitis is essential for induction of pancreatic ductal adenocarcinoma by K-Ras oncogenes in adult mice. Cancer Cell 2007;11:291–302.
7. Biankin AV, Waddell N, Kassahn KS, Gingras MC, Muthuswamy LB, Johns AL, Miller DK, Wilson PJ, Patch AM, Wu J, Chang DK, Cowley MJ, Gardiner BB, Song S, Harliwong I, Idrisoglu S, Nourse C, Nourbakhsh E, Manning S, Wani S, Gongora M, Pajic M, Scarlett CJ, Gill AJ, Pinho AV, Rooman I, Anderson M, Holmes O, Leonard C, Taylor D, Wood S, Xu Q, Nones K, Fink JL, Christ A, Bruxner T, Cloonan N, Kolle G, Newell F, Pinese M, Mead RS, Humphris JL, Kaplan W, Jones MD, Colvin EK, Nagrial AM, Humphrey ES, Chou A, Chin VT, Chantrill LA, Mawson A, Samra JS, Kench JG, Lovell JA, Daly RJ, Merrett ND, Toon C, Epari K, Nguyen NQ, Barbour A, Zeps N, Australian Pancreatic Cancer Genome I, Kakkar N, Zhao F, Wu YQ, Wang M, Muzny DM, Fisher WE, Brunicardi FC, Hodges SE, Reid JG, Drummond J, Chang K, Han Y, Lewis LR, Dinh H, Buhay CJ, Beck T, Timms L, Sam M, Begley K, Brown A, Pai D, Panchal A, Buchner N, De Borja R, Denroche RE, Yung CK, Serra S, Onetto N, Mukhopadhyay D, Tsao MS, Shaw PA, Petersen GM, Gallinger S, Hruban RH, Maitra A, Iacobuzio-Donahue CA, Schulick RD, Wolfgang CL, Morgan RA, Lawlor RT, Capelli P, Corbo V, Scardoni M, Tortora G, Tempero MA, Mann KM, Jenkins NA, Perez-Mancera PA, Adams DJ, Largaespada DA, Wessels LF, Rust AG, Stein LD, Tuveson DA, Copeland NG, Musgrove EA, Scarpa A, Eshleman JR, Hudson TJ, Sutherland RL, Wheeler DA, Pearson JV, McPherson JD, Gibbs RA, Grimmond SM. Pancreatic cancer genomes reveal aberrations in axon guidance pathway genes. Nature 2012;491:399–405.
8. Kanda M, Matthaei H, Wu J, Hong SM, Yu J, Borges M, Hruban RH, Maitra A, Kinzler K, Vogelstein B, Goggins M. Presence of somatic mutations in most early-stage pancreatic intraepithelial neoplasia. Gastroenterology 2012;142:730–733 e9.
9. Hingorani SR, Petricoin EF, Maitra A, Rajapakse V, King C, Jacobetz MA, Ross S, Conrads TP, Veenstra TD, Hitt BA, Kawaguchi Y, Johann D, Liotta LA, Crawford HC, Putt ME, Jacks T, Wright CV, Hruban RH, Lowy AM, Tuveson DA. Preinvasive and invasive ductal pancreatic cancer and its early detection in the mouse. Cancer Cell 2003;4:437–450.
10. Collins MA, Bednar F, Zhang Y, Brisset JC, Galban S, Galban CJ, Rakshit S, Flannagan KS, Adsay NV, Pasca di Magliano M. Oncogenic Kras is required for both the initiation and maintenance of pancreatic cancer in mice. J Clin Invest 2012;122:639–653.
11. Lowenfels AB, Maisonneuve P, Cavallini G, Ammann RW, Lankisch PG, Andersen JR, Dimagno EP, Andren-Sandberg A, Domellof L. Pancreatitis and the risk of pancreatic cancer. International Pancreatitis Study Group. N Engl J Med 1993;328:1433–1437.
12. Bardeesy N, DePinho RA. Pancreatic cancer biology and genetics. Nat Rev Cancer 2002;2:897–909.
13. Carriere C, Young AL, Gunn JR, Longnecker DS, Korc M. Acute pancreatitis markedly accelerates pancreatic cancer progression in mice expressing oncogenic Kras. Biochem Biophys Res Commun 2009;382:561–565.
14. Hofbauer B, Saluja AK, Lerch MM, Bhagat L, Bhatia M, Lee HS, Frossard JL, Adler G, Steer ML. Intra-acinar cell activation of trypsinogen during caerulein-induced pancreatitis in rats. Am J Physiol 1998;275:G352–G362.
15. Wei D, Wang L, Yan Y, Jia Z, Gagea M, Li Z, Zuo X, Kong X, Huang S, Xie K. KLF4 is essential for induction of cellular identity change and acinar-to-ductal reprogramming during early pancreatic carcinogenesis. Cancer Cell 2016;29:324–338.
16. Morris JP, Cano DA, Sekine S, Wang SC, Hebrok M. Beta-catenin blocks Kras-dependent reprogramming of acini into pancreatic cancer precursor lesions in mice. J Clin Invest 2010;120:508–520.
17. McAllister F, Bailey JM, Alsina J, Nirschl CJ, Sharma R, Fan H, Rattigan Y, Roeser JC, Lankapalli RH, Zhang H, Jaffee EM, Drake CG, Housseau F, Maitra A, Kolls JK, Sears CL, Pardoll DM, Leach SD. Oncogenic Kras activates a hematopoietic-to-epithelial IL-17 signaling axis in preinvasive pancreatic neoplasia. Cancer Cell 2014; 25:621–637.
18. Avraham H, Park SY, Schinkmann K, Avraham S. RAFTK/Pyk2-mediated cellular signalling. Cell Signal 2000;12:123–133.
19. Avraham S, London R, Fu Y, Ota S, Hiregowdara D, Li J, Jiang S, Pasztor LM, White RA, Groopman JE, et al. Identification and characterization of a novel related adhesion focal tyrosine kinase (RAFTK) from megakaryocytes and brain. J Biol Chem 1995;270:27742–27751.
20. Okigaki M, Davis C, Falasca M, Harroch S, Felsenfeld DP, Sheetz MP, Schlessinger J. Pyk2

regulates multiple signaling events crucial for macrophage morphology and migration. Proc Natl Acad Sci U S A 2003;100:10740–10745.
21. Jiang H, Hegde S, Knolhoff BL, Zhu Y, Herndon JM, Meyer MA, Nywening TM, Hawkins WG, Shapiro IM, Weaver DT, Pachter JA, Wang-Gillam A, DeNardo DG. Targeting focal adhesion kinase renders pancreatic cancers responsive to checkpoint immunotherapy. Nat Med 2016;22:851–860.
22. Shi G, DiRenzo D, Qu C, Barney D, Miley D, Konieczny SF. Maintenance of acinar cell organization is critical to preventing Kras-induced acinar-ductal metaplasia. Oncogene 2013;32:1950–1958.
23. Eser S, Reiff N, Messer M, Seidler B, Gottschalk K, Dobler M, Hieber M, Arbeiter A, Klein S, Kong B, Michalski CW, Schlitter AM, Esposito I, Kind AJ, Rad L, Schnieke AE, Baccarini M, Alessi DR, Rad R, Schmid RM, Schneider G, Saur D. Selective requirement of PI3K/PDK1 signaling for Kras oncogene-driven pancreatic cell plasticity and cancer. Cancer Cell 2013;23:406–420.
24. Sawey ET, Johnson JA, Crawford HC. Matrix metalloproteinase 7 controls pancreatic acinar cell transdifferentiation by activating the Notch signaling pathway. Proc Natl Acad Sci U S A 2007;104:19327–19332.
25. Esni F, Miyamoto Y, Leach SD, Ghosh B. Primary explant cultures of adult and embryonic pancreas. Methods Mol Med 2005;103:259–271.
26. Morris JP, Wang SC, Hebrok M. KRAS, Hedgehog, Wnt and the twisted developmental biology of pancreatic ductal adenocarcinoma. Nat Rev Cancer 2010;10:683–695.
27. Jones S, Zhang X, Parsons DW, Lin JC, Leary RJ, Angenendt P, Mankoo P, Carter H, Kamiyama H, Jimeno A, Hong SM, Fu B, Lin MT, Calhoun ES, Kamiyama M, Walter K, Nikolskaya T, Nikolsky Y, Hartigan J, Smith DR, Hidalgo M, Leach SD, Klein AP, Jaffee EM, Goggins M, Maitra A, Iacobuzio-Donahue C, Eshleman JR, Kern SE, Hruban RH, Karchin R, Papadopoulos N, Parmigiani G, Vogelstein B, Velculescu VE, Kinzler KW. Core signaling pathways in human pancreatic cancers revealed by global genomic analyses. Science 2008;321:1801–1806.
28. Fukuda A, Wang SC, Morris JP, Folias AE, Liou A, Kim GE, Akira S, Boucher KM, Firpo MA, Mulvihill SJ, Hebrok M. Stat3 and MMP7 contribute to pancreatic ductal adenocarcinoma initiation and progression. Cancer Cell 2011;19:441–455.
29. Corcoran RB, Contino G, Deshpande V, Tzatsos A, Conrad C, Benes CH, Levy DE, Settleman J, Engelman JA, Bardeesy N. STAT3 plays a critical role in KRAS-induced pancreatic tumorigenesis. Cancer Res 2011;71:5020–5029.
30. Baumgart S, Chen NM, Siveke JT, Konig A, Zhang JS, Singh SK, Wolf E, Bartkuhn M, Esposito I, Hessmann E, Reinecke J, Nikorowitsch J, Brunner M, Singh G, Fernandez-Zapico ME, Smyrk T, Bamlet WR, Eilers M, Neesse A, Gress TM, Billadeau DD, Tuveson D, Urrutia R, Ellenrieder V. Inflammation-induced NFATc1-STAT3 transcription complex promotes pancreatic cancer initiation by KrasG12D. Cancer Discov 2014;4:688–701.
31. Verma N, Keinan O, Selitrennik M, Karn T, Filipits M, Lev S. PYK2 sustains endosomal-derived receptor signalling and enhances epithelial-to-mesenchymal transition. Nat Commun 2015;6:6064.
32. Kapoor A, Yao W, Ying H, Hua S, Liewen A, Wang Q, Zhong Y, Wu CJ, Sadanandam A, Hu B, Chang Q, Chu GC, Al-Khalil R, Jiang S, Xia H, Fletcher-Sananikone E, Lim C, Horwitz GI, Viale A, Pettazzoni P, Sanchez N, Wang H, Protopopov A, Zhang J, Heffernan T, Johnson RL, Chin L, Wang YA, Draetta G, DePinho RA. Yap1 activation enables bypass of oncogenic Kras addiction in pancreatic cancer. Cell 2014;158:185–197.
33. Zhang W, Nandakumar N, Shi Y, Manzano M, Smith A, Graham G, Gupta S, Vietsch EE, Laughlin SZ, Wadhwa M, Chetram M, Joshi M, Wang F, Kallakury B, Toretsky J, Wellstein A, Yi C. Downstream of mutant KRAS, the transcription regulator YAP is essential for neoplastic progression to pancreatic ductal adenocarcinoma. Sci Signal 2014;7:ra42.
34. Gruber R, Panayiotou R, Nye E, Spencer-Dene B, Stamp G, Behrens A. YAP1 and TAZ control pancreatic cancer initiation in mice by direct up-regulation of JAK-STAT3 signaling. Gastroenterology 2016;151:526–539.
35. Bryant KL, Mancias JD, Kimmelman AC, Der CJ. KRAS: feeding pancreatic cancer proliferation. Trends Biochem Sci 2014;39:91–100.
36. Ardito CM, Gruner BM, Takeuchi KK, Lubeseder-Martellato C, Teichmann N, Mazur PK, Delgiorno KE, Carpenter ES, Halbrook CJ, Hall JC, Pal D, Briel T, Herner A, Trajkovic-Arsic M, Sipos B, Liou GY, Storz P, Murray NR, Threadgill DW, Sibilia M, Washington MK, Wilson CL, Schmid RM, Raines EW, Crawford HC, Siveke JT. EGF receptor is required for KRAS-induced pancreatic tumorigenesis. Cancer Cell 2012;22:304–317.
37. Ji B, Tsou L, Wang H, Gaiser S, Chang DZ, Daniluk J, Bi Y, Grote T, Longnecker DS, Logsdon CD. Ras activity levels control the development of pancreatic diseases. Gastroenterology 2009;137:1072–1082, 1082 e1-6.
38. Zhang Y, Morris JP, Yan W, Schofield HK, Gurney A, Simeone DM, Millar SE, Hoey T, Hebrok M, Pasca di Magliano M. Canonical wnt signaling is required for pancreatic carcinogenesis. Cancer Res 2013;73:4909–4922.
39. Pasca di Magliano M, Biankin AV, Heiser PW, Cano DA, Gutierrez PJ, Deramaudt T, Segara D, Dawson AC, Kench JG, Henshall SM, Sutherland RL, Dlugosz A, Rustgi AK, Hebrok M. Common activation of canonical Wnt signaling in pancreatic adenocarcinoma. PLoS One 2007;2:e1155.
40. Al-Aynati MM, Radulovich N, Riddell RH, Tsao MS. Epithelial-cadherin and beta-catenin expression changes in pancreatic intraepithelial neoplasia. Clin Cancer Res 2004;10:1235–1240.
41. Gao C, Chen G, Kuan SF, Zhang DH, Schlaepfer DD, Hu J. FAK/PYK2 promotes the Wnt/beta-catenin pathway and intestinal tumorigenesis by phosphorylating GSK3beta. Elife 2015;4.

42. Piedra J, Miravet S, Castano J, Palmer HG, Heisterkamp N, Garcia de Herreros A, Dunach M. p120 Catenin-associated Fer and Fyn tyrosine kinases regulate beta-catenin Tyr-142 phosphorylation and beta-catenin-alpha-catenin Interaction. Mol Cell Biol 2003; 23:2287–2297.
43. Saito A, Yamashita T, Mariko Y, Nosaka Y, Tsuchiya K, Ando T, Suzuki T, Tsuruo T, Nakanishi O. A synthetic inhibitor of histone deacetylase, MS-27-275, with marked in vivo antitumor activity against human tumors. Proc Natl Acad Sci U S A 1999;96:4592–4597.
44. Lilien J, Balsamo J. The regulation of cadherin-mediated adhesion by tyrosine phosphorylation/dephosphorylation of beta-catenin. Curr Opin Cell Biol 2005;17:459–465.
45. Coluccia AM, Vacca A, Dunach M, Mologni L, Redaelli S, Bustos VH, Benati D, Pinna LA, Gambacorti-Passerini C. Bcr-Abl stabilizes beta-catenin in chronic myeloid leukemia through its tyrosine phosphorylation. EMBO J 2007;26:1456–1466.
46. Sulzmaier FJ, Jean C, Schlaepfer DD. FAK in cancer: mechanistic findings and clinical applications. Nat Rev Cancer 2014;14:598–610.
47. van Veelen W, Le NH, Helvensteijn W, Blonden L, Theeuwes M, Bakker ER, Franken PF, van Gurp L, Meijlink F, van der Valk MA, Kuipers EJ, Fodde R, Smits R. beta-catenin tyrosine 654 phosphorylation increases Wnt signalling and intestinal tumorigenesis. Gut 2011;60:1204–1212.
48. White BD, Chien AJ, Dawson DW. Dysregulation of Wnt/beta-catenin signaling in gastrointestinal cancers. Gastroenterology 2012;142:219–232.
49. Aung KL, McWhirter E, Welch S, Wang L, Lovell S, Stayner LA, Ali S, Malpage A, Makepeace B, Ramachandran M, Dhani NC, Hedley DW, Knox JJ, Siu LL, Goodwin RA, Bedard PL. A phase II trial of GSK2256098 and trametinib in patients with advanced pancreatic ductal adenocarcinoma (PDAC) (MOBILITY-002 Trial, NCT02428270). J Clin Oncol 2018;36:409.
50. Schaller MD. Cellular functions of FAK kinases: insight into molecular mechanisms and novel functions. J Cell Sci 2010;123:1007–1013.
51. Weis SM, Lim ST, Lutu-Fuga KM, Barnes LA, Chen XL, Gothert JR, Shen TL, Guan JL, Schlaepfer DD, Cheresh DA. Compensatory role for Pyk2 during angiogenesis in adult mice lacking endothelial cell FAK. J Cell Biol 2008;181:43–50.
52. Lim Y, Lim ST, Tomar A, Gardel M, Bernard-Trifilo JA, Chen XL, Uryu SA, Canete-Soler R, Zhai J, Lin H, Schlaepfer WW, Nalbant P, Bokoch G, Ilic D, Waterman-Storer C, Schlaepfer DD. PyK2 and FAK connections to p190Rho guanine nucleotide exchange factor regulate RhoA activity, focal adhesion formation, and cell motility. J Cell Biol 2008;180:187–203.
53. Rustad KC, Wong VW, Gurtner GC. The role of focal adhesion complexes in fibroblast mechanotransduction during scar formation. Differentiation 2013;86:87–91.
54. Koppel AC, Kiss A, Hindes A, Burns CJ, Marmer BL, Goldberg G, Blumenberg M, Efimova T. Delayed skin wound repair in proline-rich protein tyrosine kinase 2 knockout mice. Am J Physiol Cell Physiol 2014; 306:C899–C909.
55. Lang D, Glukhov AV, Efimova T, Efimov IR. Role of Pyk2 in cardiac arrhythmogenesis. Am J Physiol Heart Circ Physiol 2011;301:H975–H983.

Received December 17, 2018. Accepted July 12, 2019.

Correspondence
Address correspondence to: Jing Hu, PhD, 2.42D, UPMC Hillman Cancer Center Research Pavilion, University of Pittsburgh School of Medicine, 5117 Centre Avenue, Pittsburgh, Pennsylvania 15213. e-mail: jih25@pitt.edu; fax: (412) 623-7828.

Author contributions
Jing Hu and Chenxi Gao conceived, designed, and analyzed the experiments; Chenxi Gao, Guangming Chen, Dennis Han Zhang, Judy Zhang, and Xuan Gao performed the experiments; Shih-Fan Kuan performed immunohistochemistry analysis of human tissue microarrays containing pancreatic ductal adenocarcinoma and pancreatic intraepithelial neoplasia; Wenhuo Hu performed bioinformatics analysis; Farzad Esni, Jun-Lin Guan, and Edward Chu provided experimental materials, discussed the results, and commented on the important intellectual content of the manuscript; and Jing Hu and Chenxi Gao wrote the manuscript.

Conflicts of interest
The authors disclose no conflicts.

Funding
This work was supported in part by National Cancer Institute grant CA166197 and CA175202 (J.H.). This project used the UPMC Hillman Cancer Center Animal Facility and Tissue and Research Pathology/Health Sciences Tissue Bank shared resource, which was supported in part by National Cancer Institute award P30CA047904.